Petroleum Science 23 (2026) 851–867

Contents lists available at ScienceDirect

Petroleum Science

journal homepage: www.keaipublishing.com/en/journals/petroleum-science

Original Paper

Enhancing acrylamide-based polymer performance in high temperature drilling fluid: Role of isopentenol polyoxyethylene ether

Yuan-Wei Sun [a,b], Jin-Sheng Sun [a,b], Kai-He Lv [a,b], Jing-Ping Liu [a,b,*], Chen-Jing Shi [a,b], Tai-Feng Zhang [a,b], Yu-Fan Zheng [a,b], Han Yan [a,b], Ye-Cheng Li [a,b]

[a] State Key Laboratory of Deep Oil and Gas, China University of Petroleum (East China), Qingdao, 266580, Shandong, China
[b] School of Petroleum Engineering, China University of Petroleum (East China), Qingdao, 266580, Shandong, China

ARTICLE INFO

Article history:
Received 9 July 2025
Received in revised form
27 October 2025
Accepted 28 October 2025
Available online 1 November 2025

Edited by Yan-Hua Sun

Keywords:
Drilling fluid
Acrylamide-based polymer
High temperature
Isopentenol polyoxyethylene ether
Synergistic mechanism

ABSTRACT

Acrylamide-based polymers have been widely applied in drilling fluids due to their excellent water solubility, structural tunability, and adaptability to various fluid systems. However, under high-temperature downhole conditions, these polymers are prone to molecular chain degradation, conformational collapse, and reduced adsorption capacity, resulting in a significant decline in rheological control and filtration loss performance. These limitations severely restrict their application in high-temperature wells. Enhancing the structural stability and functional durability of polymers under elevated temperatures has become a critical challenge in the development of high-performance drilling fluid materials. Isoprenol polyoxyethylene ether (TPEG) has been demonstrated to improve the thermal resistance of acrylamide-based polymers. Nevertheless, incorporating TPEG into polymer chains contradicts the conventional design paradigm that seeks to eliminate thermally labile structures in high-temperature-resistant polymers. Therefore, elucidating the microscopic mechanisms by which TPEG modulates polymer chain evolution, conformational behavior, thermal degradation pathways, and adsorption characteristics at elevated temperatures is essential to understanding its synergistic effect. In this study, isoprenol polyoxyethylene ether (the most commonly used type with a molecular weight of 2400 was chosen, TPEG-2400) was introduced into a DMAA/AMPS acrylamide-based copolymer system and systematically compared with conventional DMAA/AMPS binary copolymers. The incorporation of TPEG-2400 significantly enhanced the thermal conformational stability and clay adsorption capacity of the polymer, enabling the drilling fluid to retain favorable rheological and filtration properties even after aging at 220 °C. The mechanism of action was elucidated by correlating changes in the physicochemical properties of the polymer with the analysis of its thermal degradation products. The highly flexible polyether structure was found to hinder interchain entanglement and coiling, while the strongly hydrophilic polyether segments formed a robust hydration layer, increasing electrostatic repulsion between clay particles. Moreover, the polyether chains may exhibit a “self-sacrificing” behavior under high-temperature conditions, preferentially decomposing to protect key functional groups such as amide moieties from thermal damage. This cooperative effect, from both conformational and thermodynamic perspectives, contributes to delaying polymer failure. It is concluded that the functional behavior of the segment structure plays a more significant role than its intrinsic thermal stability in enhancing the effective operating temperature of acrylamide-based polymers in drilling fluids. This counterintuitive yet strategically effective approach—introducing structurally specific but thermally less stable segments to achieve performance enhancement—offers a novel design perspective for future development of high-temperature-resistant polymer additives in drilling fluids.

1. Introduction

In oil and gas drilling operations, drilling fluids play multiple critical roles, including cuttings transport, bit cooling, borehole stabilization, and formation pressure control (Balaga and Kulkarni,

* Corresponding author.
E-mail address: liujingping20@126.com (J.-P. Liu).
Peer review under the responsibility of China University of Petroleum (Beijing).

https://doi.org/10.1016/j.petsci.2025.10.028

2022). To meet the increasingly complex demands of deep wells and ultra-deep wells, the composition of drilling fluids has been continuously refined and optimized (Song et al., 2023). As essential modifiers within drilling fluid systems, polymer additives are extensively employed to regulate rheology and control fluid loss (Davoodi et al., 2024). Among them, acrylamide-based polymers have gained wide application in high-temperature freshwater, brine, and high-density drilling fluids due to their excellent water solubility, structural designability, and strong adaptability (Gautam et al., 2022). However, acrylamide-based polymers suffer from insufficient structural stability under high-temperature conditions. Their backbones and side chains are susceptible to thermal degradation, coiling, or desorption, leading to molecular weight reduction, conformational changes, and a consequent decline in viscosity and filtration control capabilities (Li et al., 2024). Enhancing the structural stability and functional durability of these polymers under elevated temperatures has become a technical challenge and research focus in the development of high-performance drilling fluids. In recent years, researchers have attempted to improve the thermal resistance of polymers from the perspective of molecular design by introducing monomers bearing steric hindrance or functional groups, thereby constructing copolymer segment structures with special conformational or interfacial interaction capabilities (Noor et al., 2025).

Isoprenol polyoxyethylene ether (TPEG) is a nonionic polyether monomer featuring a hydrophobic allyl alcohol group and hydrophilic polyether chains. It possesses intrinsic molecular weight and exhibits excellent water solubility and dispersion stability. In the materials industry, the most commonly used variant is TPEG-2400, which has a molecular weight of 2400 and is widely utilized in the synthesis of polycarboxylate superplasticizers. As one of the most prevalent monomers for water reducers, TPEG-2400 enhances the dispersion and fluidity of cement/concrete systems by forming a stable steric hindrance layer through its flexible polyether side chains adsorbed onto cement particle surfaces, thereby suppressing flocculation and aggregation (Zuo et al., 2017). Owing to its outstanding dispersibility and adsorption performance, TPEG-2400 has recently been introduced into the development of polymer additives for drilling fluids (Sun et al., 2024b). Its polyether structure offers high hydrophilicity and chain flexibility, which theoretically enhances the conformational stability of the polymer in aqueous environments while forming stable adsorption layers on clay particles such as bentonite (Zhang et al., 2020), thus improving the rheological behavior and filter cake quality of the drilling fluid (Sun et al., 2021). Yang J. et al. (2023, 2024) incorporated TPEG into acrylamide-based copolymers to synthesize a comb-shaped polymer fluid loss reducer with thermal resistance up to 220 °C (Yang J. et al., 2024) and a comb-shaped polymer/nano-lithium saponite composite rheology regulator with thermal resistance up to 240 °C (Yang J. et al., 2023). Liu L. M. et al. (2022a, 2022b) copolymerized TPEG with DMAA and AMPS to prepare a fluid loss reducer capable of withstanding 200 °C and high salinity conditions. The above-mentioned TPEG treatment agent has been industrialized and applied in some important ultra-deep well drilling projects, showing good results (Sun et al., 2024b). However, these studies primarily confirmed that TPEG-2400 can enhance the thermal resistance of polymers, while mechanistic understanding remains limited to structural modification and enhanced clay interaction stability. Moreover, the polyether segment itself is thermally labile, beginning to degrade at around 180 °C, which contradicts the traditional design philosophy of avoiding weak bond structures in high-temperature-resistant polymers. To date, a systematic investigation into how TPEG modulates polymer chain evolution, conformational transformation, thermal degradation pathways, and adsorption behavior under high temperatures remains lacking.

This study focuses on the performance and underlying mechanisms by which TPEG-2400 enhances the functionality of acrylamide-based polymers in high-temperature drilling fluids. TPEG-2400 was introduced into a *N*,*N*-dimethylacrylamide/2-acrylamido-2-methylpropanesulfonic acid (DMAA/AMPS) copolymer system via free-radical polymerization to construct a structurally regular ternary copolymer, PDAT. Its segment structure, thermal stability, drilling fluid performance, and interaction mechanism with bentonite were systematically evaluated. Comparative studies with the conventional binary copolymer PDA (DMAA/AMPS) were conducted to investigate the influence of TPEG-2400 on polymer performance. The results indicated that the introduction of TPEG-2400 did not significantly alter the molecular weight of the polymer but substantially enhanced its conformational stability under high-temperature conditions, clay adsorption capacity, and ability to maintain drilling fluid rheology and filtration performance. Under aging at 220 °C, the PDAT-containing drilling fluid still exhibited favorable shear consistency and dense filter cake formation, significantly outperforming the control polymer without TPEG. The mechanism was innovatively elucidated by combining physicochemical characterization of the polymer with thermal degradation product analysis. The highly flexible segment structure of TPEG-2400 inhibited interchain entanglement and coiling, while the strongly hydrophilic polyether chains formed a robust hydration shell, increasing electrostatic repulsion between clay particles. The polyether segments may exhibit a “self-sacrificial” behavior under high-temperature conditions, preferentially decomposing to protect critical functional groups such as amide moieties from thermal damage. From both conformational and thermodynamic perspectives, such a mechanism synergistically delays polymer failure.

It is concluded that the functional role of the segment structure contributes more significantly than its intrinsic thermal stability to enhancing the effective temperature range of acrylamide-based polymers in drilling fluids. As current research on improving the high-temperature resistance of these polymers approaches a bottleneck, this strategically counterintuitive enhancement strategy—introducing thermally less stable yet functionally effective segment structures—may represent a promising new design pathway for future high-performance polymer additives in high-temperature drilling fluids.

2. Experiments and materials

2.1. Materials

N,*N*-Dimethylacrylamide (DMAA, AR), 2-acrylamido-2-methylpropanesulfonic acid (AMPS, AR), isopentenol polyoxyethylene ether with a molecular weight of 2400 (TPEG-2400, AR), sodium hydroxide (NaOH, AR), ammonium persulfate ($(NH_4)S_2O_8$, AR) were purchased from Sinopharm Chemical Reagent Company. The bentonite used to prepare drilling fluid was purchased from Huaian County Tengfei Bentonite Company.

2.2. Experiments

Fig. 1 shows the overall flowchart of the experiment conducted in this study, which can be divided into four parts. The purple part represents the synthesis and purification of the polymer, the orange part represents the characterization of the polymer, the blue part represents the configuration and performance evaluation of

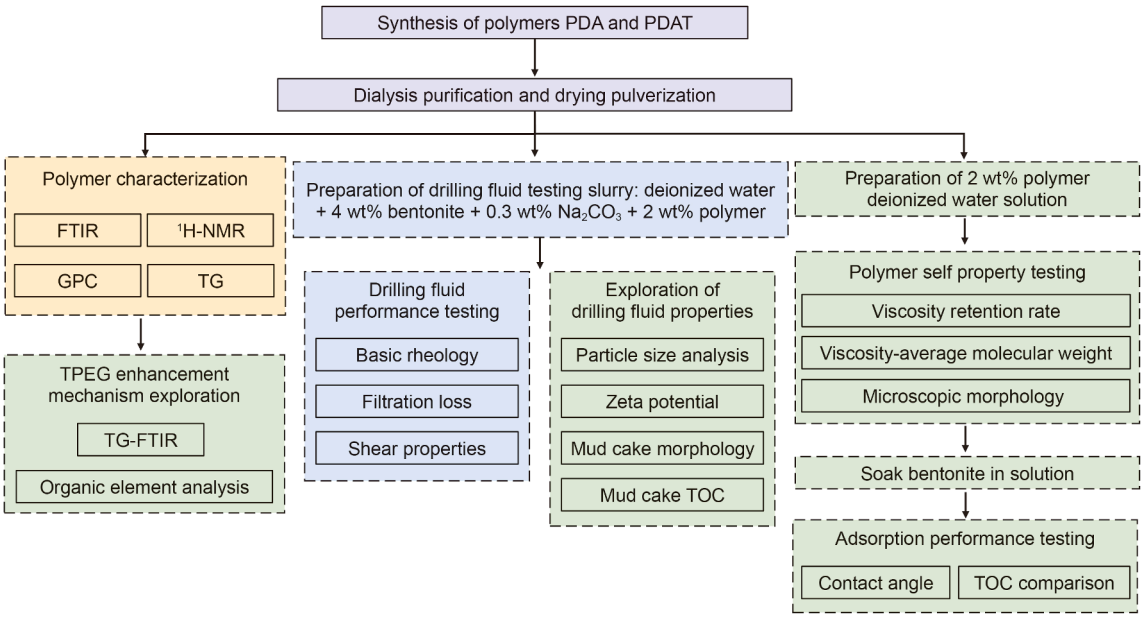

Fig. 1. Overall flowchart of the study.

the drilling fluid test slurry, and the green part represents the mechanism research experiment.

2.2.1. Preparation of polymers

Equal masses of the monomers DMAA and AMPS were weighed and dissolved in deionized water under continuous stirring until complete dissolution was achieved. NaOH was then added dropwise to adjust the pH of the solution to 7–8. The resulting solution was transferred to a three-necked flask, deoxygenated by purging with nitrogen gas, and subsequently heated to 65 °C in a thermostatic water bath. A 10 wt% solution of $(NH_4)_2S_2O_8$ was added dropwise to initiate the polymerization reaction. The reaction was maintained at 65 °C for 4 h. Upon completion, the resulting gel product was transferred into a dialysis bag and purified by dialysis against deionized water for 48 h. The purified product was then dried and ground to obtain the binary copolymer PDA composed of DMAA and AMPS. In the above reaction system, the total monomer mass accounted for 25 wt% of the solvent, and the initiator $(NH_4)_2S_2O_8$ was used at 0.5 wt% relative to the total monomer mass. Following the same procedure, the ternary copolymer PDAT was synthesized by additionally introducing TPEG-2400 at 10 wt% of the combined mass of DMAA and AMPS into the reaction system. The synthesis procedures and theoretical segment structures of PDA and PDAT are illustrated in Fig. 2(a).

2.2.2. Characterization of polymers

To characterize the chemical structures of PDA and PDAT, Fourier-transform infrared spectroscopy (FTIR) was performed using the potassium bromide pellet method in the range of 400–4000 cm^{-1}, and proton nuclear magnetic resonance (^1H NMR) spectroscopy was conducted after dissolving the polymers in deuterium oxide. The molecular weight information of the polymers was obtained via aqueous-phase gel permeation chromatography (GPC) and intrinsic viscosity measurement using an Ubbelohde viscometer. Thermal stability and decomposition behavior were investigated through thermogravimetric analysis coupled with infrared spectroscopy (TG-FTIR) in the range of 30–600 °C and 400–4000 cm^{-1}. To assess the thermal resistance of the polymers, 2 wt% aqueous polymer solutions were sealed in metal aging cells and subjected to thermal aging at various temperatures for 16 h. The aged samples were then freeze-dried, and their morphologies were examined using scanning electron microscopy (SEM). Elemental changes in the polymers after thermal aging were analyzed using organic elemental analysis. Before conducting the above tests, the instruments were calibrated in advance and strictly tested according to the reproducible testing program developed in the instruments. The final results obtained through data processing methods such as averaging or transformation were analyzed to ensure the objectivity of the results.

2.2.3. Polymer performance test

A 4 wt% bentonite-based drilling fluid slurry was prepared (under stirring, add 4 wt% bentonite to deionized water, followed by 0.3 wt% sodium carbonate to promote sodium activation and enhance the hydration and dispersion of bentonite.), into which 2 wt% of PDA or PDAT was separately added. The mixtures were stirred at 11,000 rpm for 20 min and then subjected to thermal aging at various temperatures to obtain test slurries. The plastic viscosity (PV), yield point (YP), initial gel strength (G_{10s}) and 10-min gel strength (G_{10min}) of the drilling fluids were measured using a six-speed rotational viscometer, and the rheological parameters were calculated after obtaining stable values according to the method specified in Chinese standard GB/T 16783.1-2014 (Qu et al., 2024). A HAAKE rheometer was employed to determine the shear stress at different shear rates and the complex modulus under varying shear stress conditions. The shear rate increased from the minimum detectable value of the instrument to 100 s^{-1} and the shear stress increased from 0.01 to 100 Pa. Filtration loss was measured in accordance with API standard procedures (Li et al., 2025). The API filtration loss (FL_{API}) is obtained by cooling the aged test slurry to room temperature and testing it under a pressure difference of 0.69 MPa and the high temperature and high pressure filtration loss (FL_{HTHP}) is measured at the corresponding aging temperature under a pressure difference of 3.45 MPa. The API filter cake was dried and sputter-coated with gold, and its microstructure was then observed by SEM. Changes in zeta potential and clay particle size distribution with temperature were characterized using a zeta potential analyzer and a laser particle

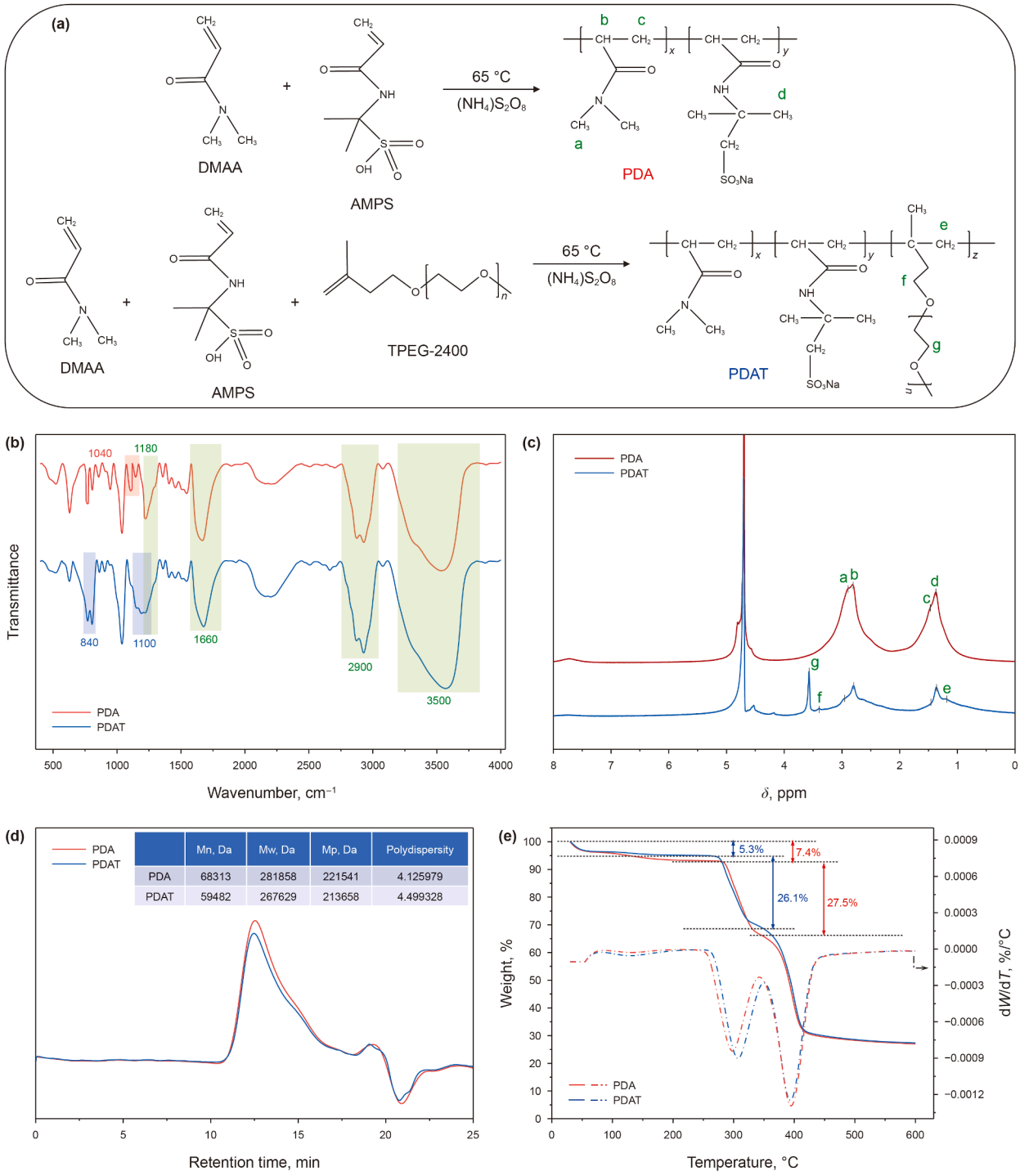

Fig. 2. Synthesis route, theoretical structure and characterization of PDA and PDAT: (**a**) synthesis route and theoretical structural formula, (**b**) FTIR spectra, (**c**) ^{1}H-NMR spectra, (**d**) GPC curves, (**e**) TG curves.

size analyzer according to the same repeatable program, respectively. To evaluate the temperature-dependent adsorption behavior of the polymers on clay, bentonite was dispersed into 2 wt% deionized aqueous solutions of the polymers aged at different temperatures. After soaking for 24 h, the suspensions were centrifuged, and the lower-layer precipitates were collected, dried, and subjected to total organic carbon (TOC) analysis. Contact angle measurements were performed on the pressed precipitates to further characterize the adsorption capacity of the polymers on clay under different thermal conditions.

3. Results and discussion

3.1. Characterization of polymers

3.1.1. Chemical structure

Fig. 2(b) presents the FTIR spectra of PDA and PDAT. The broad absorption band around 3500 cm^{-1} corresponds to the N–H stretching vibration of amide groups. The peak at approximately 2900 cm^{-1} is attributed to the C–H stretching vibrations of methyl and methylene groups (Huo et al., 2018). The peak at 1660 cm^{-1}

corresponds to the C=O stretching vibrations of tertiary and secondary amides (Luo et al., 2023). The absorption band at 1180 cm^{-1} represents the asymmetric stretching vibration of the sulfonic acid group (S=O) (Sun et al., 2022). These characteristic peaks originate from DMAA and AMPS and are observed in both PDA and PDAT. Due to the incorporation of TPEG-2400, the FTIR spectrum of PDAT exhibits a new out-of-plane CH_2 rocking vibration peak at 840 cm^{-1} and a strong C–O–C stretching vibration peak at 1100 cm^{-1} (Yan et al., 2013). The intensity of the C–O–C peak is so pronounced that it even overlaps the symmetric S=O stretching peak at 1040 cm^{-1} (Wang R. et al., 2024), highlighting the structural differences between PDA and PDAT.

Fig. 2(c) displays the ^1H NMR spectra of both polymers. Four characteristic peaks are observed in both PDA and PDAT: peak a ($\delta = 2.92$) corresponds to the $–CH_3$ protons adjacent to the nitrogen atom in DMAA; peaks b ($\delta = 2.80$) and c ($\delta = 1.47$) correspond to –CH and $–CH_2$ protons on the DMAA main chain, respectively (Bai et al., 2023); peak d ($\delta = 1.37$) is assigned to the $–CH_3$ protons in AMPS (Tang et al., 2016). In addition, several new peaks appear in the NMR spectrum of PDAT: peak e ($\delta = 1.19$) corresponds to the $–CH_2$ protons in the TPEG-2400 backbone; peak f ($\delta = 3.38$) represents the characteristic signal of $–OCH_3$ groups; and peak g ($\delta = 3.57$) is attributed to the repeating $–O–CH_2–CH_2–O–$ units of the polyoxyethylene ether chain (Lin et al., 2024). The appearance of these additional peaks confirms the successful incorporation of TPEG-2400 into the PDAT structure.

Combining the FTIR and ^1H NMR analyses, it is evident that the actual molecular structures of PDA and PDAT are consistent with the theoretical segment structures shown in Fig. 2(a), confirming the successful synthesis of the copolymers.

3.1.2. Molecular weight

For polymer additives used in drilling fluids, molecular weight plays a decisive role in determining their performance, such as dispersibility, viscosity enhancement, and thermal stability (Dong et al., 2024). Generally, monomers with bulky steric hindrance—such as sodium *p*-styrene sulfonate and *N*-vinylpyrrolidone—tend to impede polymer chain growth to some extent, thereby increasing the difficulty of synthesizing high-molecular-weight polymers (Jiang et al., 2019).

Fig. 2(d) shows the elution curves of PDA and PDAT obtained from GPC analysis, revealing similar trends for both polymers. Molecular weight statistics indicate that the number-average molecular weight (Mn), weight-average molecular weight (Mw), and peak molecular weight (Mp) of PDA and PDAT are approximately the same, with PDAT exhibiting a slightly lower molecular weight. The polydispersity index (PDI) of PDAT increases only marginally compared to that of PDA. These results suggest that the introduction of TPEG-2400 has a negligible effect on the molecular weight of the acrylamide-based polymer, and the steric hindrance posed by TPEG-2400 is significantly lower than that of other bulky monomers, which is beneficial for synthesizing polymers with higher molecular weights (Gautam et al., 2025). Moreover, the similar molecular weights of PDA and PDAT minimize the influence of molecular weight differences on performance, ensuring a fair comparison in subsequent drilling fluid performance evaluations.

3.1.3. Thermal stability

Fig. 2(e) shows the thermogravimetric (TG) curves of PDA and PDAT, which reveal similar overall weight loss behavior. The minor weight loss observed below 100 °C is attributed to the evaporation of residual free water present in the samples (Xie et al., 2023). Between 100 and 280 °C, the mass loss occurs gradually, which can be ascribed to the decomposition of thermally labile groups and the evaporation of bound water associated with strongly hydrophilic groups such as amide and sulfonic acid moieties. A more pronounced weight loss is observed between 280 and 380 °C, indicating the onset of functional group breakdown within the polymer chains (Minakov et al., 2023). During this stage, side chains and some segments of the main chain begin to degrade. Above 380 °C, the polymers enter the main chain decomposition and carbonization phase, where rapid mass loss occurs, ultimately yielding carbonaceous residues (Mao et al., 2021). A comparison of the two curves shows that although the incorporation of TPEG-2400 does not significantly alter the onset temperatures of the individual decomposition stages, it reduces the extent of mass loss prior to the main chain degradation stage. This observation suggests that TPEG-2400 may enhance the thermal resistance of the polymer to some extent. Moreover, the introduction of polyether segments could potentially modify the degradation process and the resulting decomposition products, which will be discussed in greater detail in the subsequent TG-FTIR analysis section.

3.2. Impact on drilling fluid

3.2.1. Rheological performance

Rheological performance is one of the most fundamental properties of drilling fluids. A favorable rheological profile enables the drilling fluid to effectively suspend solid particles (Gao et al., 2025), clean the borehole bottom, enhance the rate of penetration, and maintain a regular wellbore geometry, thereby ensuring drilling safety (Sun et al., 2019).

Fig. 3(a) illustrates the variation in plastic viscosity of drilling fluid test slurries containing PDA and PDAT as a function of aging temperature. Maintaining appropriate and stable viscosity is essential for safe and efficient drilling operations. Before aging, the plastic viscosity of the two slurries were similar. As the aging temperature increased, the plastic viscosity gradually decreased due to polymer desorption and thermal degradation. However, the decline in PDAT slurry was significantly less pronounced. At 220 °C, the plastic viscosity of the PDAT slurry decreased by only about 33%, whereas that of the PDA slurry dropped by more than 50%. Across all aging temperatures, the plastic viscosity of the PDAT slurry remained higher than that of the PDA slurry.

Fig. 3(b) presents the changes in yield point of both slurries with increasing aging temperature. The yield point reflects the strength of the network structure formed by clay particles, which is directly related to the cuttings-carrying capacity of the drilling fluid (Zheng et al., 2020). With increasing temperature, the yield point of the PDA slurry decreased sharply, indicating breakdown of its structural network; at 220 °C, the yield point dropped to only 2 Pa. In contrast, the PDAT slurry exhibited a more moderate decline, retaining a yield point of 6 Pa at 220 °C—three times higher than that of PDA—demonstrating superior cuttings transport capability.

The initial gel strength (G_{10s}) and 10-min gel strength (G_{10min}) are key rheological parameters that reflect the ability of the drilling fluid to build and maintain a structural network under static conditions. The initial gel strength (measured after 10 s of static aging) indicates the rate at which the polymer–clay network structure reforms when fluid motion stops, representing the immediate interparticle interactions. The final gel strength (measured after 10 min of static aging) reflects the degree of structural consolidation and the strength of the three-dimensional network formed by hydrated clay particles and adsorbed polymer chains over time. Higher gel strengths generally correspond to a more robust and stable network structure, which is essential for suspending cuttings during circulation interruptions and maintaining wellbore stability at elevated temperatures (Wisniowski

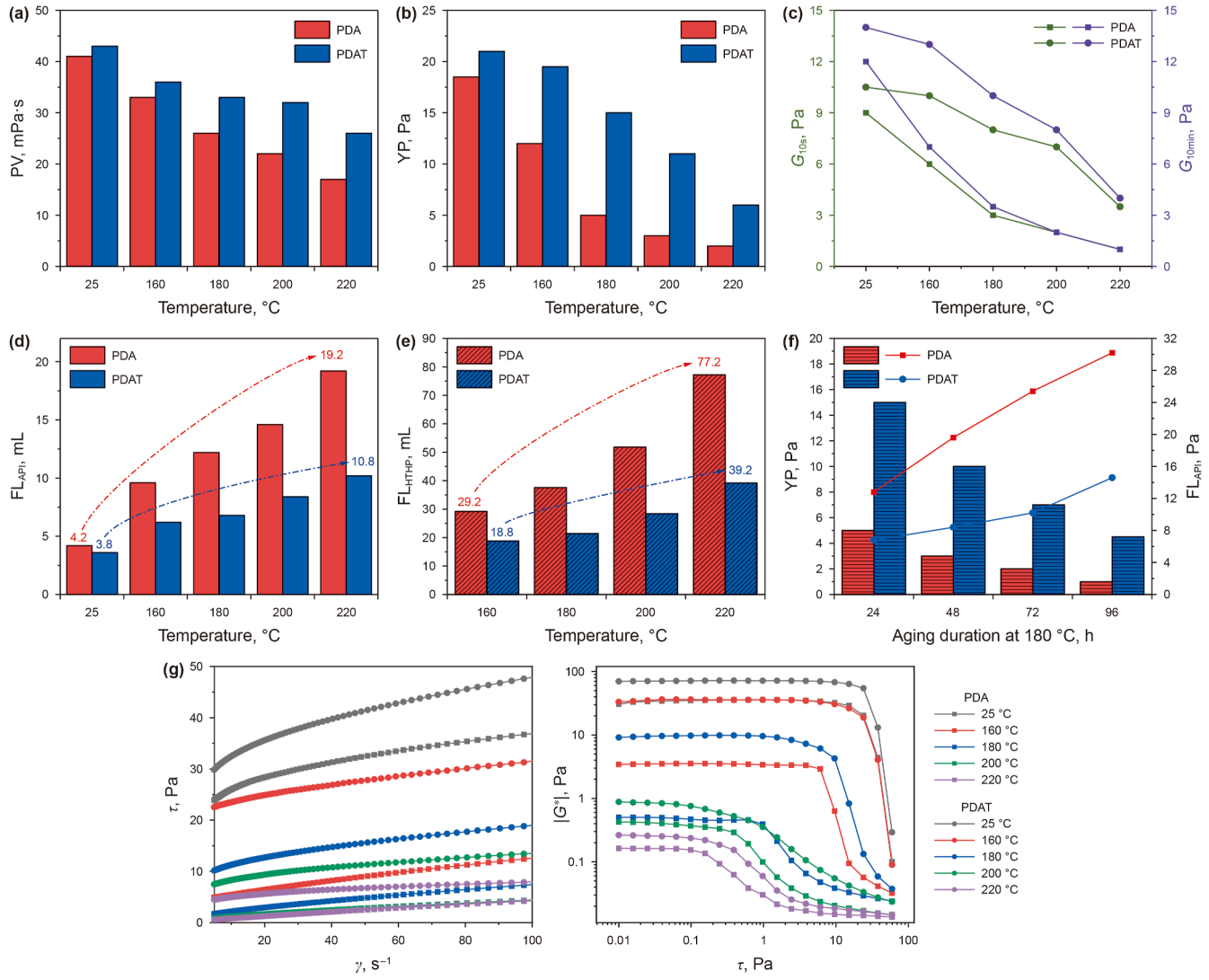

Fig. 3. Effect of PDA and PDAT on rheological filtration performance of drilling fluid: (**a**) plastic viscosity (PV), (**b**) yield point (YP), (**c**) initial gel strength (G_{10s}) and 10-min gel strength (G_{10min}), (**d**) API filtration loss (FL_{API}), (**e**) HTHP filtration loss (FL_{HTHP}), (**f**) long term aging performance, (**g**) shear properties.

et al., 2020). According to Fig. 3(c), it can be seen that the G_{10s} and G_{10min} of PDAT test slurry are always greater than PDA after aging at different temperatures, indicating that its grid structure has stronger strength.

Fig. 3(g) shows the variation of shear stress with shear rate and the change in complex shear modulus |*G**| with shear stress for the aged slurries. As the shear rate increases, the shear stress also increases, displaying the behavior of a plastic fluid. It can be seen that the rheological mode of all tested slurries approximates between Bingham mode and power-law mode. Analysis based on the Bingham model, a minimum stress, known as the static shear force, is required to initiate flow by breaking the flocculated bentonite network (Sun et al., 2023). The PDAT slurry consistently exhibited a higher static shear force than the PDA slurry. Above 180 °C, the static shear force of PDA slurry nearly vanished, while the PDAT slurry still retained a measurable static shear force even after aging at 220 °C, indicating a more robust internal network structure. Before reaching the critical stress threshold, |*G**| remained nearly constant with increasing stress. A sharp drop in |*G**| at the critical stress indicated disruption of the network structure among clay particles (Wang et al., 2012). After high-temperature aging, the critical stress of the PDAT slurry remained substantially higher, suggesting that its internal structure was more stable and better suited for high-temperature environments.

These results collectively demonstrate that the incorporation of TPEG-2400 effectively enhances the ability of the copolymer to maintain rheological stability of the drilling fluid under elevated temperatures.

3.2.2. Filtration performance

Filtration is another critical performance parameter for drilling fluids. An effective drilling fluid should be capable of rapidly forming a thin yet robust filter cake, minimizing fluid invasion into the formation, and thereby maintaining wellbore stability and drilling safety (Zhong et al., 2020).

Fig. 3(d) illustrates the changes in API filtration volume (FL_{API}) of PDA and PDAT slurries at various aging temperatures. As the aging temperature increases, the FL_{API} rises continuously, which is largely attributed to polymer desorption and degradation, leading to a gradual loss of protective interactions with clay particles. However, the PDAT slurry exhibited a significantly smaller increase in filtration volume. From room temperature to 220 °C, the FL_{API} increased from 3.8 to 10.8 mL, while for the PDA slurry, it rose

sharply from 4.2 to 19.2 mL. High-temperature and high-pressure filtration (FL_{HTHP}) tests are widely used to evaluate the fluid loss performance of drilling fluids under extreme conditions. Compared to FL_{API} at ambient conditions, FL_{HTHP} better simulates the actual downhole environment, where the drilling fluid is subjected to elevated temperatures and high confining pressures. Fig. 3(f) shows the FL_{HTHP} of different test slurries at corresponding aging temperatures. It can be seen that the FL_{HTHP} of PDAT test slurry is significantly lower, and the high-temperature and high-pressure filtration loss of PDAT test slurry at 220 °C is only about half of that of PDA test slurry.

This clearly indicates that the copolymer containing TPEG-2400 exhibits superior filtration control capability under high-temperature conditions. This improvement can be attributed to multiple factors, including enhanced clay particle dispersion and more stable adsorption behavior (Chen et al., 2018), which will be analyzed in greater detail in the subsequent mechanism discussion section.

3.2.3. Long-term aging performance

Long-term aging tests are essential for evaluating the thermal stability and durability of drilling fluid additives under extended exposure to high-temperature environments. In real drilling operations, particularly in deep and ultra-deep wells, the circulation time of drilling fluids can last for several days or even weeks, during which the additives are continuously subjected to elevated temperatures, pressure, and complex chemical environments.

According to Fig. 3(b) and (d), it can be seen that the performance of PDA test slurry deteriorates severely after aging at 220 °C for 16 h. Continuing to age at 220 °C for a long time cannot reflect the process of performance degradation with increasing aging time. In order to objectively compare the performance changes of PDA and PDAT under long-term aging conditions, 180 °C was selected as the long-term aging temperature. Fig. 3(f) shows the performance of PDA and PDAT test slurries after aging at 180 °C for 24, 48, 72, and 96 h, respectively. It can be seen that as the aging time increases, the yield point of the test slurry decreases and the FL_{API} increases, indicating that the network structure composed of polymer and clay in the drilling fluid is gradually destroyed and polymer gradually fails. However, the performance degradation rate and amplitude of PDAT test slurry are significantly smaller. After 96 h of aging, the yield point value of the drilling fluid is still 5 Pa, and the filtration loss is still acceptable. This indicates that the introduction of TPEG delays the damage of high temperature to the polymer, making the polymer have better long-term temperature resistance.

3.3. Mechanism analysis

3.3.1. Changes of copolymer properties at high temperatures

For polymer additives used in drilling fluids, the failure temperature often does not directly correlate with the TG curve (Sun et al., 2024a). Instead, factors such as conformational stability and dispersion state under high temperatures play a significant role in determining polymer performance—yet these factors are not readily reflected in TG analysis. Changes in the physicochemical properties of polymers under high-temperature conditions are fundamental to performance deterioration. When dispersed in aqueous systems, polymer chains may undergo curling, scission, and other structural transitions at elevated temperatures, resulting in changes in molecular weight and morphology. The stability of these properties can to some extent reflect the retention of polymer functionality.

Fig. 4(a) shows the plastic viscosity and viscosity retention of 2 wt% polymer aqueous solutions after aging at different temperatures. With increasing aging temperature, the viscosity of the solutions decreased sharply, which can be attributed to configurational and conformational changes such as chain coiling and degradation. Comparing PDA and PDAT, the viscosity retention of PDAT was consistently higher. The difference was most pronounced at 180 °C, where PDAT retained about 20% of its original viscosity, while PDA retained less than 10%. Even at 220 °C, PDAT still exhibited approximately 10% viscosity retention, suggesting less conformational collapse of its molecular chains under high-temperature conditions.

Fig. 4(b) presents the viscosity-average molecular weight (Mv) of the polymers, measured using an Ubbelohde viscometer (Koh et al., 2022). Before aging, both polymers exhibited similar Mv values. Upon thermal aging, the Mv of PDA dropped sharply, falling to less than 10% of its original value at 180 °C, indicating severe hydrolysis and structural breakdown, leaving it incapable of resisting further thermal damage. In contrast, the Mv of PDAT decreased more gradually with temperature. At 180 °C, it retained about 45% of its initial molecular weight, and even with further heating, the polymer still showed a degree of resistance to thermal degradation, indicating a residual structural integrity in its molecular chains.

Polymer solutions aged at 25 (ambient), 180, and 220 °C were freeze-dried and analyzed via scanning electron microscopy (SEM) to observe their morphologies. As shown in Fig. 4(c), at ambient temperature, both polymers were well dispersed in solution and exhibited distinct network structures. Due to its comb-like molecular structure, the PDAT copolymer with TPEG-2400 formed a visibly coarser and more robust network, which physically hindered chain entanglement. As previously analyzed, 180 °C appears to be a critical temperature at which notable differences between the two polymers emerge. SEM images confirmed this: PDA chains showed significant entanglement, distortion, and degradation, with their morphology transforming from a defined network into fragmented sheets, blocks, and filaments—indicating severe structural damage (Oya and Kawakatsu, 2014). Although some chain entanglement was also observed in PDAT, the overall network framework remained visible, suggesting that its primary structure was still largely preserved. When the aging temperature was increased to 220 °C, the morphology of PDA had completely transitioned into indistinct amorphous clusters with no discernible network features. Although the PDAT chains also underwent substantial morphological changes at this temperature, portions of the original network skeleton were still observable, correlating with its higher residual molecular weight.

The introduction of polyether structures imparts highly flexible side chains with large conformational entropy to the polymer. According to Kramers' rate theory, this results in a higher entropic barrier for chain curling under thermal agitation (Pollak and Miret-Artes, 2023), favoring the maintenance of an extended and open conformation at elevated temperatures. Consequently, the polymer chains are less prone to rapid or intense collapse under high-temperature conditions (Bacosca et al., 2012). These structural advantages are not readily captured in TG curves, offering a direct explanation for the discrepancy between the similar thermal degradation profiles and the divergent high-temperature performance of the two polymers.

3.3.2. Effect of copolymer on particle size and dispersion of clay

At elevated temperatures, the hydration layer on clay particles in drilling fluids becomes thinner, and the electrostatic repulsion between particles weakens. This reduction in repulsive force decreases the dispersion stability of the clay, leading to particle agglomeration and an increase in particle size (Mech and Sangwai, 2016). As a result, the pore size of the filter cake enlarges and the

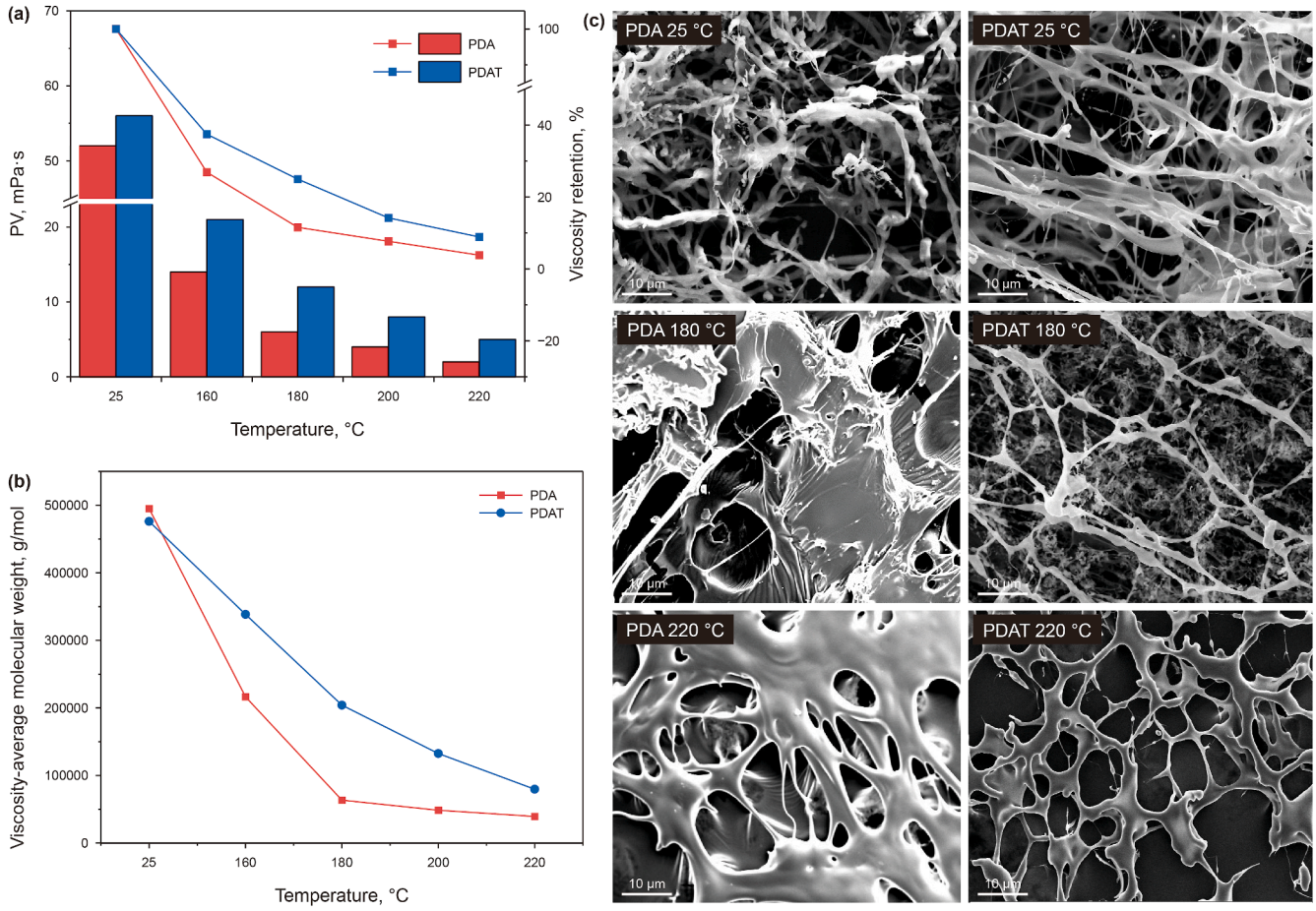

Fig. 4. Changes of copolymer properties after aging at different temperatures: (**a**) plastic viscosity and viscosity retention (2 wt% solutions), (**b**) viscosity-average molecular weight, (**c**) microscopic morphology.

fluid loss increases. Polymer additives can adsorb onto the clay surface, offering a protective effect that helps maintain moderate dispersion of the particles and enhances the overall performance of the drilling fluid.

Fig. 5(a) presents the particle size distribution curves of PDA and PDAT slurries after thermal aging at different temperatures. Before aging, both slurries showed relatively concentrated particle size distributions, though with relatively large particle sizes overall. This is likely due to the formation of network structures within the drilling fluid, which prevent the laser particle size analyzer from resolving individual clay particles. In such cases, the instrument may interpret network aggregates as single large particles. The slightly larger particle size observed in the PDAT slurry is likely a result of greater polymer adsorption and a more robust network structure. After thermal aging, the particle size distribution broadened. The smaller-sized fraction represents well-dispersed clay, which is essential for maintaining favorable rheological and filtration properties. In contrast, the larger-sized fraction (> 100 μm) corresponds to thermally agglomerated clay, which exhibits poor dispersion, low contribution to viscosity and yield strength, and forms looser filter cakes. The occurrence of such large particles should be minimized. Across all temperatures, the PDAT slurries consistently retained a higher proportion of well-dispersed clay compared to those with PDA. Even after aging at 200 °C, the majority of clay particles in the PDAT slurry remained in a reasonable size range. Although some agglomeration was observed at 220 °C, the distribution was still concentrated in the functional range. In contrast, the PDA slurry displayed a pronounced peak in the particle size distribution above 100 μm, indicating severe agglomeration. Fig. 5(b) further illustrates the changes in median particle diameter (D_{50}) with increasing aging temperature. The PDA slurry exhibited a sharp increase in median particle size, while the PDAT slurry maintained a relatively stable size distribution up to 200 °C. Even at 220 °C, 50% of the particles in the PDAT slurry remained smaller than 15 μm.

Zeta potential reflects the potential difference between the adsorbed and diffuse layers of clay particles and serves as a key indicator of colloidal dispersion stability (Cui and van Duijneveldt, 2010). A higher absolute value of zeta potential indicates stronger electrostatic repulsion between particles and greater dispersion stability. Both PDA and PDAT are anionic polymers that, when adsorbed onto the clay surface, increase the surface negative charge, thicken the hydration shell, and strengthen interparticle repulsion, thereby enhancing clay dispersion (Greesh et al., 2008). As shown in Fig. 5(c), the absolute value of zeta potential decreased with increasing temperature, indicating that the polymers on the clay surface had undergone desorption or degradation, weakening their protective effect. At all temperatures, the absolute value of zeta potential for the PDAT slurry remained higher than that of PDA, and the difference between them widened with temperature. This suggests that the incorporation of TPEG-2400 enhances the adsorption and protective effects of the copolymer on clay surfaces and improves its functional stability at high temperatures. The polyether chains possess strong hydrophilicity and tend to extend outward into the aqueous phase (Zhong et al., 2015), forming a thick and stable hydration film that inhibits clay agglomeration and helps

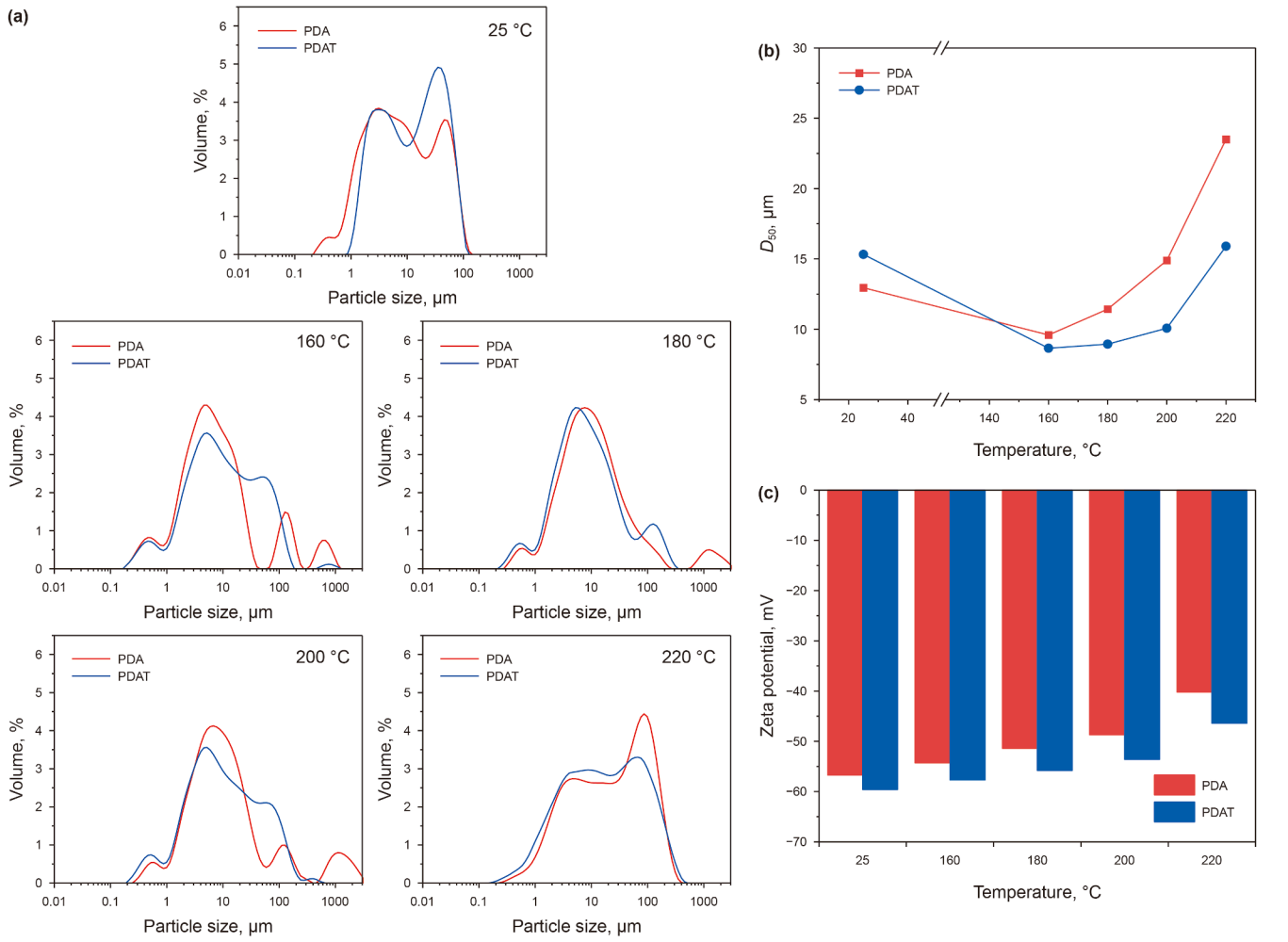

Fig. 5. Particle size distribution and zeta potential of clay particles after aging at different temperatures: (**a**) particle size distribution, (**b**) D_{50}, (**c**) zeta potential.

maintain the polymer-clay network structure in the drilling fluid (Liu, 2007).

3.3.3. *Effect of copolymer on mud cake of drilling fluid*

Both PDA and PDAT contain amide groups that facilitate adsorption onto clay surfaces, while sulfonic acid groups enhance clay hydration, thereby promoting the formation of dense filter cakes in drilling fluids (Wang D.-Y. et al., 2024). Fig. 6 presents the macroscopic and microscopic morphologies of the filter cakes formed by PDA and PDAT slurries after aging at various temperatures. Before thermal aging, both filter cakes appeared thin and smooth on the macroscopic scale. Microscopically, their surfaces were flat and compact, with no visible pores or fissures, indicating that the polymers had effectively adsorbed onto the clay surfaces and were functioning as intended (Wang et al., 2013). As the aging temperature increased, the macroscopic appearance of the filter cakes became progressively rougher and thicker. After aging at 160 °C, visible pores began to appear on the surface of the PDA filter cake, and with further temperature increase, the filter cake became increasingly populated with large aggregated clay particles and enlarged pores. These morphological changes are a direct cause of the sharp increase in fluid loss. In contrast, the filter cakes formed by PDAT slurries remained relatively dense after thermal aging. Even after aging at 200 °C, the filter cake surface remained smooth, flat, and compact, with almost no large particle aggregates observed under SEM. Although some degree of clay agglomeration was evident at 220 °C, the structural integrity of the PDAT filter cake remained superior to that of the PDA counterpart. These results demonstrate that the copolymer containing TPEG-2400 retains its ability to adsorb onto clay surfaces under high-temperature conditions (Wang et al., 2022), contributing to the formation of high-quality filter cakes and thereby improving the fluid loss control performance of the drilling fluid (Obi et al., 2024).

3.3.4. *Evaluation of copolymer adsorption capacity*

Under high-temperature conditions, both polymers and clays in drilling fluids undergo complex physicochemical transformations. The adsorption and desorption behavior of polymers on clay surfaces is influenced by multiple factors (Wu et al., 2018). A commonly used evaluation method involves centrifuging aged slurries and collecting the bottom sediment for total organic carbon (TOC) analysis. Since the bentonite matrix is essentially carbon-free, the TOC content in the sediment can be used as an approximate indicator of the amount of polymer adsorbed on the clay at various temperatures (Xiong et al., 2015). As shown in Fig. 7(a), the TOC content decreases with increasing temperature, indicating reduced polymer adsorption on clay surfaces. A comparison of PDA and PDAT slurries shows that the TOC content in the PDAT sediment remains consistently higher, suggesting that PDAT has better adsorption capability under high-temperature conditions.

However, this method neglects the fact that clay itself undergoes property changes at elevated temperatures. Studies have

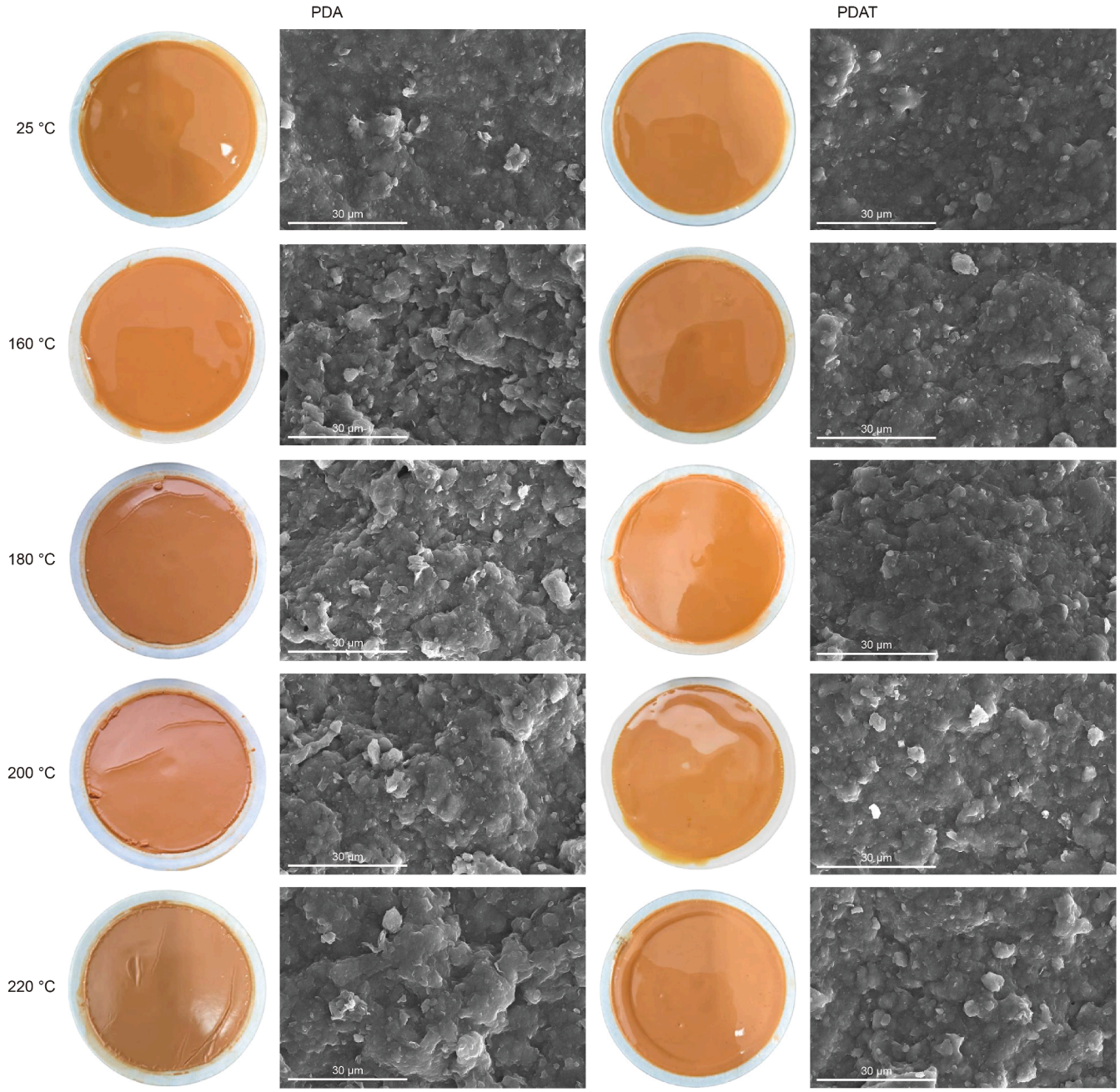

Fig. 6. Mud cakes formed by PDA and PDAT test slurries after aging at different temperatures.

shown that high-temperature exposure can passivate clay, altering its surface hydrogen bonding and specific surface area, which significantly affects polymer adsorption (Liu J.P. et al., 2022). Thus, this method may not objectively reflect the intrinsic adsorption performance of the polymers. To minimize the influence of thermally induced changes in clay properties, a modified approach was adopted: untreated bentonite was dispersed into polymer solutions aged at different temperatures, and the mixtures were incubated for 24 h at room temperature. The bottom sediment was then collected by centrifugation and subjected to TOC testing, allowing a more objective comparison of polymer adsorption on clay over a fixed time period.

To ensure the objectivity of the TOC-based adsorption comparison, the TOC content of each aged polymer solution was measured prior to sediment testing. As shown in Fig. 7(b), the TOC content of the polymer solutions showed minimal variation across aging temperatures; the TOC content of the solution aged at 220 °C was only 0.2 mg/mL lower than that of the unaged solution. Additionally, the TOC levels of PDA and PDAT solutions were comparable, suggesting that the differences observed in the sediment TOC content primarily result from differences in polymer adsorption. Fig. 7(c) presents the TOC results of the sediments obtained from these solutions. The TOC values from PDAT solutions were consistently higher than those from PDA solutions, and the gap widened as the aging temperature increased. Furthermore, PDAT exhibited a minor reduction in TOC content with temperature, indicating superior and more stable adsorption capacity at elevated temperatures.

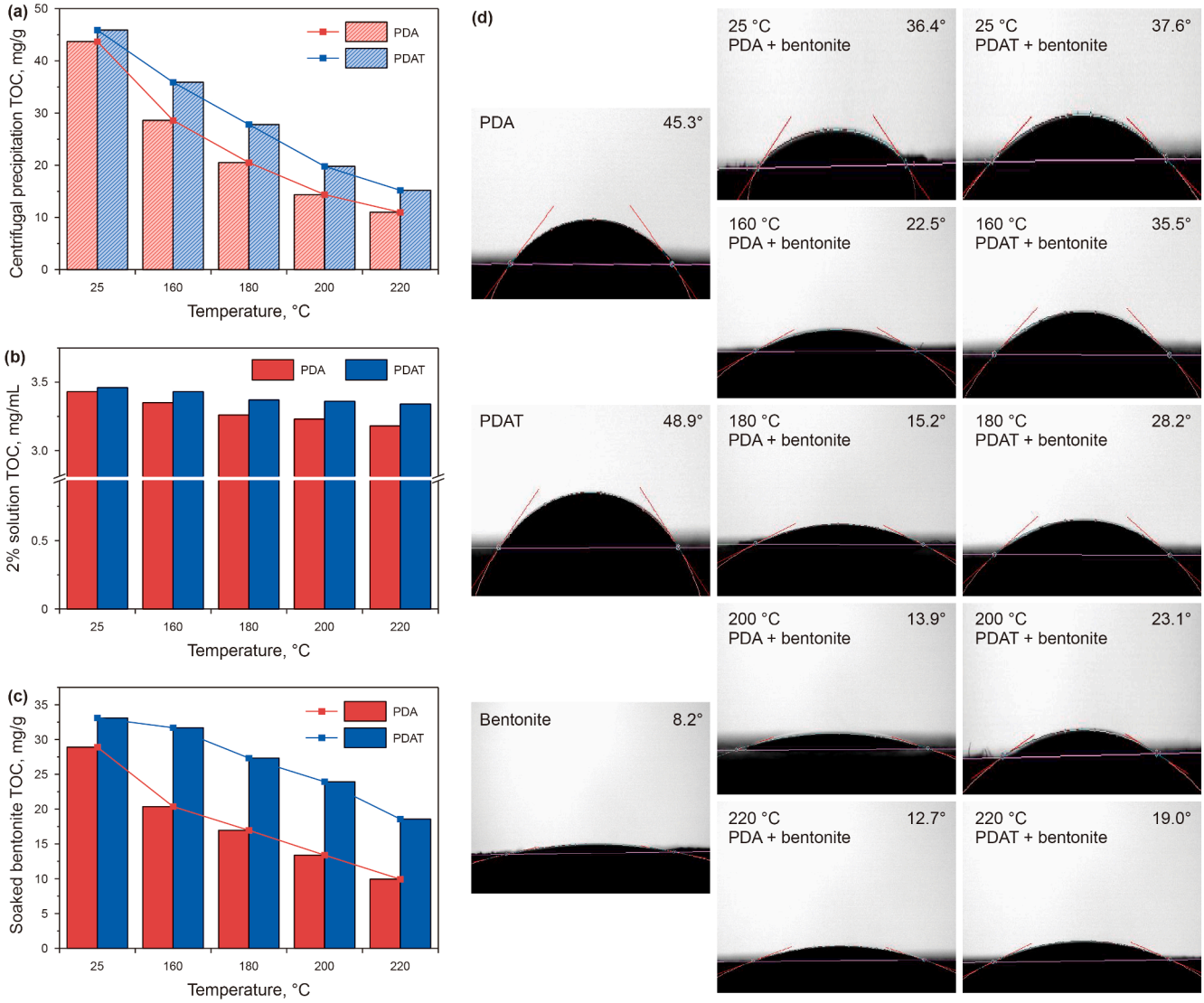

Fig. 7. Results of adsorption capacity related tests. TOC content of slurries' centrifugal precipitates (**a**), 2% solutions (**b**), and soaked bentonite (**c**); (**d**) contact angles.

To further visualize the difference in adsorption behavior, the sediment from each polymer solution was dried and pressed into thin wafers, and the water contact angle of each surface was measured, and the results are shown in Fig. 7(d). For reference, pressed wafers of bentonite, PDA, and PDAT powders were also tested. The pure bentonite wafer exhibited strong hydrophilicity, with a contact angle of only 8.2°, while PDA and PDAT powders showed contact angles of 45.3° and 48.9°, respectively, due to their relatively lower surface hydrophilicity. Adsorption of polymer onto clay increases the contact angle; thus, greater adsorption is theoretically correlated with a higher contact angle (Yao et al., 2022). Before thermal aging, the contact angles of PDA- and PDAT-treated wafers increased significantly compared to pure bentonite, indicating good adsorption of both polymers, consistent with the similar TOC values. After aging at 160 °C, a notable difference emerged: the contact angle of the PDA-treated wafer dropped to 22.5°, suggesting that high temperature severely weakened PDA's adsorption capacity. In contrast, the PDAT-treated wafer retained a contact angle of 35.5°, close to the unaged condition. As the temperature further increased, contact angles for both polymers declined, reflecting reduced adsorption. However, the contact angles for PDAT-treated wafers remained significantly higher than those of PDA, confirming that the introduction of TPEG-2400 enhanced the resistance of polymers to thermally induced desorption and improved its adsorption on clay surfaces in high-temperature drilling fluids.

3.3.5. *Exploration of thermal decomposition products of copolymers*

An interesting phenomenon can be observed from the above analyses: although the TGA curves and the TOC content in solution show only slight differences between the two polymers, their adsorption behavior on clay and performance in drilling fluids differ significantly. The polyether segments introduced by TPEG-2400 can extend into the aqueous phase and form hydrogen bonds with clay surfaces, thereby enhancing the adsorption ability to some extent. However, the mass of TPEG-2400 in the reaction system accounts for only 10% of the total monomer mass; the polymer backbone remains predominantly composed of DMAA and AMPS, and the thermal resistance of the polyether segment itself is limited. Therefore, its direct contribution to maintaining the polymer's adsorption capacity at high temperatures may not be substantial.

To investigate the fundamental reasons why TPEG-2400 enhances the high-temperature performance of acrylamide-based

polymers in drilling fluids, thermogravimetric-infrared (TG-FTIR) analysis was employed to examine the thermal decomposition products of PDA and PDAT, providing further insight into their degradation processes. TG-IR allows for real-time infrared spectral detection of decomposition products during thermal analysis (Ju et al., 2024). The obtained IR spectra can be used to identify the composition of volatiles released at different temperatures, thereby improving understanding of various thermal degradation stages. Fig. 8(a) presents the TG-IR results for PDA and PDAT, where the *X*-, *Y*-, and *Z*-axes represent infrared wavelength, temperature, and absorbance, respectively.

It can be observed that the two polymers exhibit similar characteristic peaks in their decomposition products, with a large quantity of volatiles detected only after 250 °C. This indicates the onset of extensive decomposition of functional groups, as well as the cleavage of side chains and portions of the main chain (Xie et al., 2024). However, PDA starts releasing large quantities of decomposition products at around 255 °C, while for PDAT, this temperature is delayed to approximately 268 °C. Moreover, PDA shows higher infrared peak intensities, suggesting a more intense decomposition process. Prior to the detection of major volatiles, some weak IR signals are already present, corresponding to the decomposition of thermally labile groups. These peaks are mainly located in the range of 1000–1700 cm^{-1}. A comparison of the spectra reveals that PDAT exhibits an additional absorption peak at 1150 cm^{-1}, likely associated with the evolution of short-chain ethers. This implies that differences may exist between the two polymers in their early-stage thermal degradation pathways.

To further compare the decomposition behavior of the two polymers, several representative infrared wavelengths were selected, and intensity–temperature curves were plotted to analyze the evolution of specific decomposition products at different temperatures (Zang et al., 2025). Among them, 1150 cm^{-1} is a key wavelength, as the characteristic peak at this position can originate from both short-chain ethers (C–O–C) produced by the degradation of polyether segments and sulfur-containing species (SO_2, $-SO_3^-$) released during sulfonic group decomposition (Zhang and Cao, 2019). Given that the decomposition temperature of sulfonic groups is typically much higher than that of polyethers, the contribution of these two processes can be distinguished. The decomposition of sulfonic groups often accompanies the breakdown of the polymer backbone. Therefore, analyzing the variation in the intensity at this wavelength offers preliminary insight into the polymer degradation mechanism. The characteristic peak at 1650 cm^{-1} mainly arises from N–H species generated during the decomposition of amide groups (Al-Muntasheri et al., 2008). Amide functionalities are important for polymer adsorption on clay surfaces. In the early stages of heating, dehydration reactions may occur, followed by Hofmann degradation at higher temperatures (Lin et al., 2019). These processes reduce the polymer's adsorption capacity. Thus, examining the evolution of this peak helps elucidate changes in adsorption performance.

As shown in Fig. 8(b), a distinct peak appears between 180 and 300 °C in the 1150 cm^{-1} curve for PDAT, indicating the release of decomposition products containing C–O–C groups (Lattimer and Williams, 2002). In contrast, no such peak is observed for PDA within this temperature range. Meanwhile, a significant peak appears in the 1650 cm^{-1} curve for PDA, suggesting the release of N–H species due to amide group degradation. For PDAT, the first major peak at 1650 cm^{-1} appears around 270 °C, significantly later than that of PDA. This suggests that in the range of 180–300 °C, the polyether segments introduced by TPEG-2400 undergo preferential degradation, thereby protecting the amide groups via a "self-sacrificial" mechanism and preserving their structure at elevated temperatures. As the temperature continues to rise, both polymers exhibit strong peaks in the 1150 and 1650 cm^{-1} curves between 350 and 450 °C, corresponding to extensive decomposition of sulfonic and amide groups, and the cleavage of side and main chains. Comparing the two polymers, the absorbance intensity for PDAT is markedly lower, and the peak in the 1650 cm^{-1} curve appears at a higher temperature. This may be attributed to the polyether segments introduced by TPEG-2400, which increase the overall molecular disorder. The flexible and long side chains act as spatial arms, raising the entropic barrier for chain coiling under thermal stress (Xu et al., 2016). Additionally, the hydrated shell formed by polyether chains imposes a kinetic anchoring effect, improving the conformational stability of the polymer (Jamadagni et al., 2009). The disruption of such conformations consumes part of the energy input (Pollak, 2024), thereby enhancing the thermal tolerance of the molecular chains.

To verify the validity of the proposed "self-sacrifice" mechanism involving ether linkages, elemental analysis was performed on the polymers before and after thermal aging at 180 and 220 °C to quantify elemental composition changes. Under high temperatures, some amide groups hydrolyze into carboxylic acids, leading to a decrease in nitrogen content, while carbon, hydrogen, and sulfur content may increase due to concentration effects (Yang X.J. et al., 2024). However, the degradation of polyether chains would result in a reduction in carbon and hydrogen content. As shown in Fig. 8(c), the relative changes in elemental composition after aging at 180 and 220 °C compared with the unaged polymers are consistent with the prior analysis. The nitrogen content decreases, while other elements generally increase. However, PDAT exhibits a significantly smaller increase in carbon and hydrogen content, and a minor decrease in nitrogen content, than PDA. Meanwhile, the increase in sulfur content—unrelated to the decomposition of ether or amide groups—remains similar for both polymers (Liu L. M. et al., 2022b), supporting the hypothesis that less amide decomposition occurred in PDAT. This suggests that the degradation of polyether segments partially replaced that of amide groups. The trend is more pronounced at 220 °C. Due to the preferential release of hydrogen-rich volatiles from polyether degradation (Matsuoka et al., 2012), PDAT shows a markedly smaller increase in hydrogen content compared with PDA. The smaller decrease in nitrogen content further confirms that fewer amide groups were degraded in PDAT. Meanwhile, this self-sacrificing speculation can also be verified in the viscosity-average molecular weight analysis described in Fig. 4(b). As the aging temperature increases, the molecular weight change of PDAT becomes smaller, indicating that the degree of damage to its main structure is smaller. These results validate, to some extent, the hypothesis of ether group "self-sacrifice." Such a mechanism of sacrificial enhancement may provide a new strategy for improving the thermal resistance of polymers designed for use in drilling fluids.

3.3.6. Mechanism analysis summary

Based on the above experimental results and analyses, the enhancement mechanism of TPEG-2400 for acrylamide-based copolymers in high-temperature drilling fluids can be summarized as shown in Fig. 9. The main mechanisms are as follows.

(1) The introduction of flexible polyether side chains with high steric hindrance and conformational entropy increases the molecular disorder of the polymer chains. This physically prevents excessive proximity and entanglement between adjacent main chain segments or different polymer chains. Under high-temperature conditions, chain segment coiling requires overcoming a greater entropic energy barrier, and polymer chains tend to adopt a more extended and open conformation. This enlarges the effective interaction area of

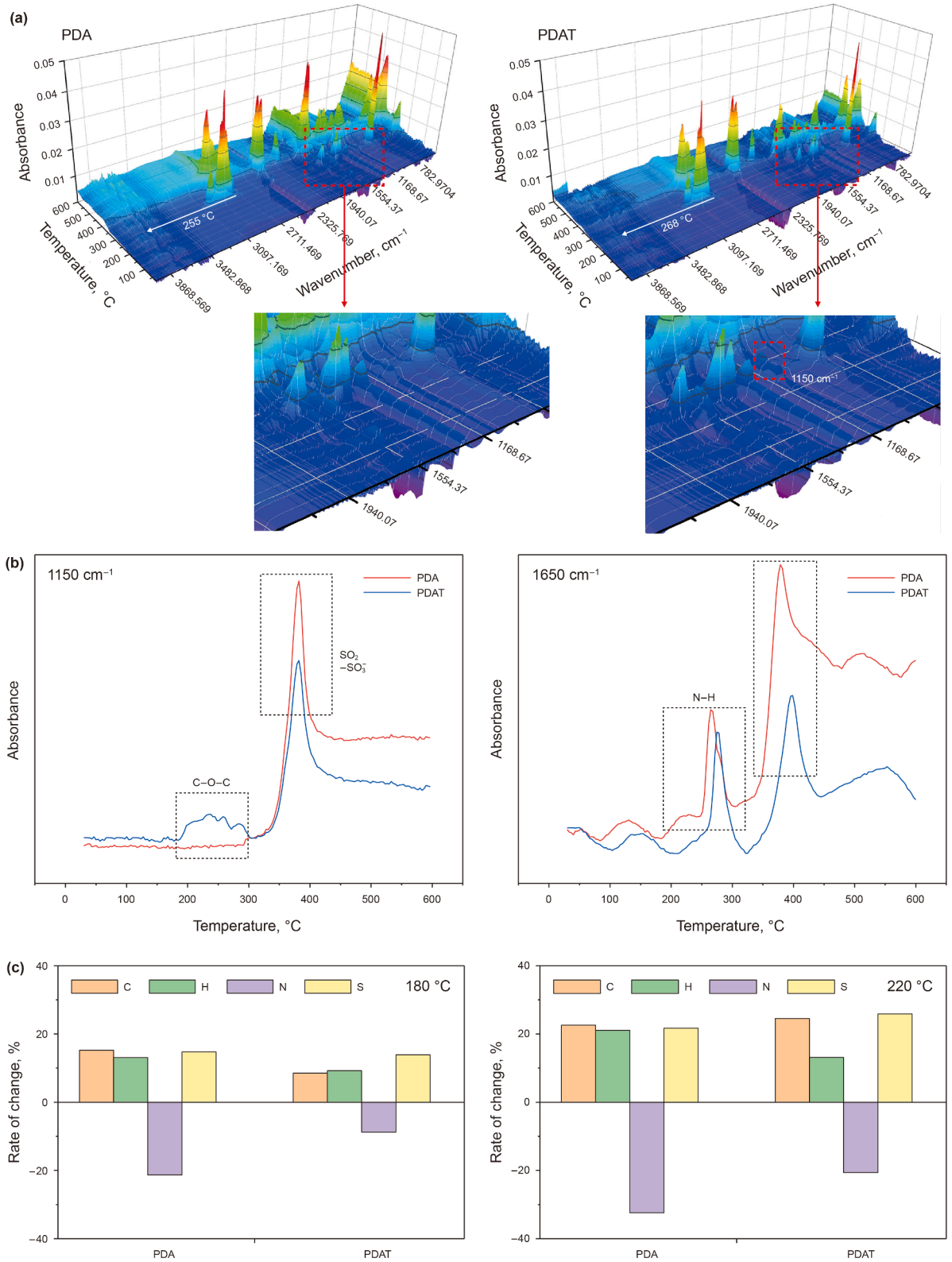

Fig. 8. Exploration of thermal decomposition products of copolymers: (**a**) TG-FTIR spectra, (**b**) variations of characteristic peaks at 1150 and 1650 cm^{-1} with temperature, (**c**) rate of change in elemental content of polymers after aging.

the molecular chains and reduces the likelihood of sudden or severe unfavorable coiling induced by intensified thermal motion, thereby enhancing the intrinsic thermal resistance of the polymer.

(2) The highly hydrophilic polyether chains extend outward into the aqueous phase in solution, forming a thick and stable hydration shell that enhances electrostatic repulsion between clay particles, improving their colloidal dispersion

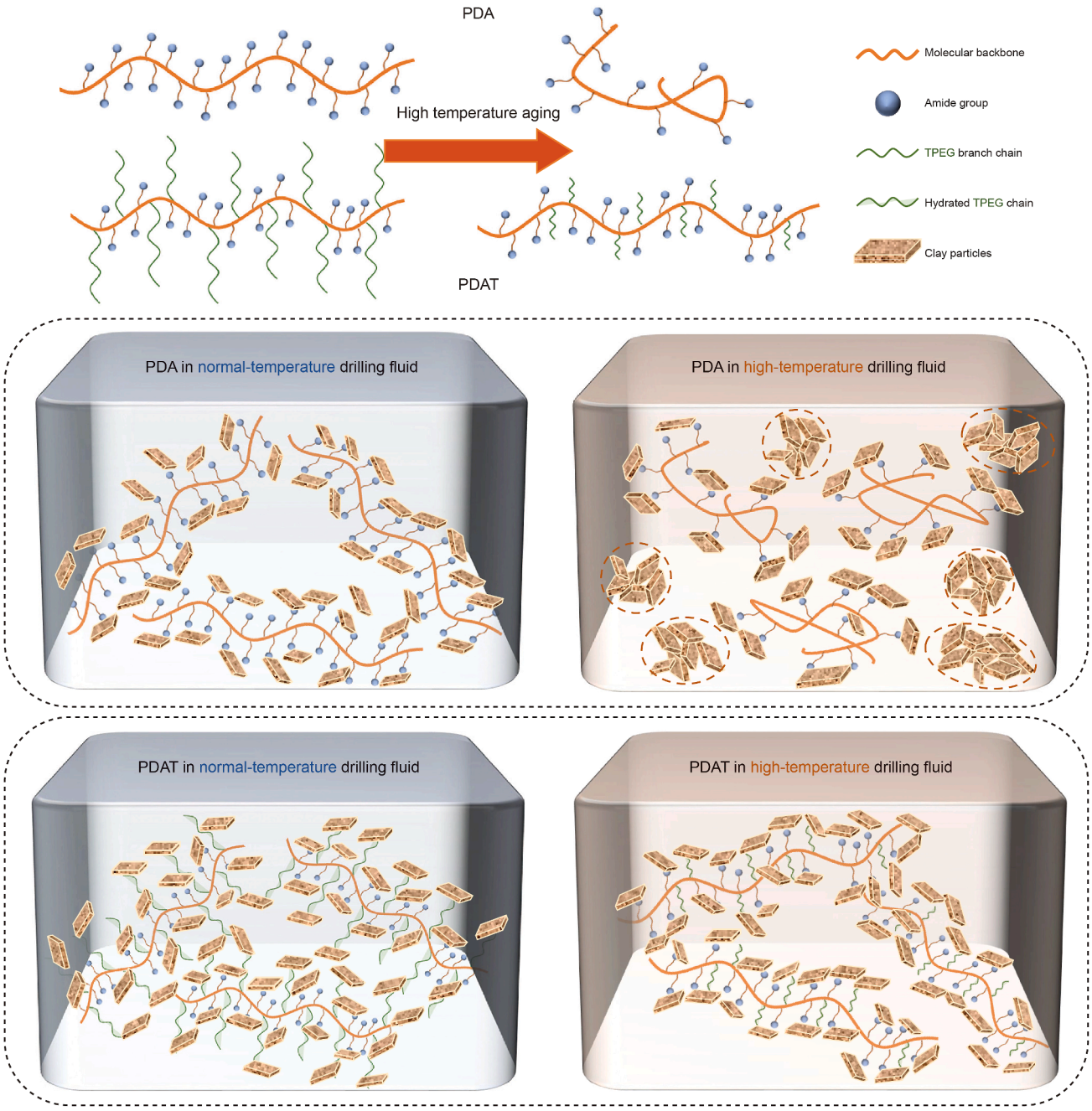

Fig. 9. Enhancing mechanism schematic diagram of TPEG.

stability and preventing aggregation. This helps maintain the polymer–clay network structure under high temperatures, enabling the aged drilling fluid to still form a thin and compact filter cake. Consequently, the introduction of polyether chains enhances the polymer's ability to stabilize the rheological and filtration properties of the drilling fluid at elevated temperatures.

(3) At lower temperatures, the polyether chains form hydrogen bonds with the clay surface, improving the polymer's adsorption capacity. At higher temperatures, the polyether segments preferentially degrade, possibly providing a "self-sacrificing" effect that protects the amide groups from thermal destruction. This allows the amide functionalities to persist at higher temperatures, maintaining the polymer's adsorption onto clay and thereby preserving its protective function. Macroscopically, this results in a noticeable increase in the effective temperature limit at which the polymer remains functional in drilling fluid systems.

4. Conclusions

(1) Isoprenol polyoxyethylene ether (TPEG-2400) exhibits excellent compatibility with acrylamide-based polymers used in drilling fluids. It can be smoothly copolymerized with commonly used monomers such as DMAA and AMPS, without significantly affecting the molecular weight of the resulting copolymer.

(2) TPEG-2400 can effectively enhance the adsorption capacity of acrylamide-based polymers onto clay in drilling fluids under high-temperature conditions. This facilitates the maintenance of the polymer–clay network structure at elevated temperatures, allowing the aged drilling fluid to still form thin and compact filter cakes, thereby improving the polymer's ability to stabilize the rheological and filtration properties of drilling fluids at high temperatures.
(3) The enhancement mechanism of TPEG-2400 for acrylamide-based copolymers in high-temperature drilling fluids can be summarized in three aspects:
   (i) The introduction of flexible polyether side chains with high steric hindrance and conformational entropy prevents polymer chain entanglement and coiling, helping maintain an extended and open conformation that increases the interaction area of molecular chains at high temperatures.
   (ii) The strongly hydrophilic polyether chains form thick hydration layers, which enhance the electrostatic repulsion between clay particles and improve their colloidal dispersion stability.
   (iii) The polyether segments enhance adsorption through hydrogen bonding with clay and may degrade preferentially at high temperatures, thereby protecting the polymer backbone and amide groups from thermal decomposition. This enables the polymer to retain its adsorption capability and protective function toward clay, leading to an extended upper temperature limit for effective performance.
(4) The functional role of specific structural units may, in some cases, contribute more to increasing the effective temperature resistance of acrylamide-based polymers in drilling fluids than their intrinsic thermal stability. Introducing structurally weaker yet functionally beneficial segments can raise the effective temperature range. The special functionality of such structures, particularly their ability to protect critical groups through sacrificial degradation, may not manifest as an increase in decomposition temperature on thermogravimetric curves, yet significantly enhances polymer performance. This strategically counterintuitive enhancement strategy—introducing thermally less stable yet functionally effective segment structures—may represent a promising new design pathway for future high-performance polymer additives in high-temperature drilling fluids.
(5) This study has identified a new pathway that is fundamentally different from the existing mechanism of enhancing the thermal resistance of drilling fluid polymers. It seems to be able to be used simultaneously with traditional efficiency enhancing pathways (such as introducing cyclic rigid monomers). We hope that future research will further expand on this concept by exploring alternative flexible side chains, multifunctional groups with enhanced interfacial interactions, and the synergistic application of such polymers with other advanced additives under ultra-high-temperature and high-salinity conditions. These efforts could pave the way for the next generation of high-performance drilling fluid polymers with superior adaptability and efficiency.

CRediT authorship contribution statement

Yuan-Wei Sun: Writing – original draft, Conceptualization. **Jin-Sheng Sun:** Investigation. **Kai-He Lv:** Resources, Investigation. **Jing-Ping Liu:** Methodology, Funding acquisition. **Chen-Jing Shi:** Data curation. **Tai-Feng Zhang:** Formal analysis. **Yu-Fan Zheng:** Visualization. **Han Yan:** Validation. **Ye-Cheng Li:** Data curation.

Declaration of interest statement

We declare that we have no financial and personal relationships with other people or organizations that can inappropriately influence our work, there is no professional or other personal interest of any nature or kind in any product, service and/or company.

Acknowledgment

This work was supported by the National Natural Science Foundation of China (52322401, 52288101).

Nomenclature

DMAA	*N*,*N*-Dimethylacrylamide
AMPS	2-Acrylamido-2-methylpropanesulfonic acid
TPEG	Isopentenol polyoxyethylene ether
TPEG-2400	Isopentenol polyoxyethylene ether with a molecular weight of 2400
PDA	AMPS/DMAA copolymer
PDAT	AMPS/DMAA/TPEG-2400 copolymer

References

Al-Muntasheri, G.A., Nasr-El-Din, H.A., Peters, J.A., Zitha, P.L.J., 2008. Thermal decomposition and hydrolysis of polyacrylamide-co-tert-butyl acrylate. Eur. Polym. J. 44 (4), 1225–1237. https://doi.org/10.1016/j.eurpolymj.2008.01.022.
Bacosca, I., Hamciuc, E., Bruma, M., Ronova, I.A., 2012. Comparative study of polyimides containing different flexible linkages. J. Iran. Chem. Soc. 9 (6), 901–910. https://doi.org/10.1007/s13738-012-0107-2.
Bai, X., Li, K., Hu, H., Yan, Y., Luo, Y., 2023. Synthesis and properties of poly (acrylamide-co-N-vinylpyrrolidone-co-sodium p-styrene sulfonate) as an anionic fluid loss additive. J. Polym. Res. 30 (5). https://doi.org/10.1007/s10965-023-03558-0.
Balaga, D.K., Kulkarni, S.D., 2022. A review of synthetic polymers as filtration control additives for water-based drilling fluids for high-temperature applications. J. Petrol. Sci. Eng. 215. https://doi.org/10.1016/j.petrol.2022.110712.
Chen, G., Lei, J., Du, Y., Du, X., Chen, X., 2018. A polycarboxylate as a superplasticizer for montmorillonite clay in cement: Adsorption and tolerance studies. Arab. J. Chem. 11 (6), 747–755. https://doi.org/10.1016/j.arabjc.2017.12.027.
Cui, Y., van Duijneveldt, J.S., 2010. Adsorption of polyetheramines on montmorillonite at high pH. Langmuir 26 (22), 17210–17217. https://doi.org/10.1021/la103278v.
Davoodi, S., Al-Shargabi, M., Wood, D.A., Rukavishnikov, V.S., Minaev, K.M., 2024. Synthetic polymers: A review of applications in drilling fluids. Pet. Sci. 21 (1), 475–518. https://doi.org/10.1016/j.petsci.2023.08.015.
Dong, X., Sun, J., Huang, X., Lv, K., Geng, Y., Liu, F., Wang, Z., Zhang, X., 2024. Development of temperature- and salt-resistant viscosifier with dual skeleton structure of microcrosslinking and hydrophobic association structures and its application in water-based drilling fluids. Colloids Surf. A Physicochem. Eng. Asp. 684. https://doi.org/10.1016/j.colsurfa.2023.133017.
Gao, S., Lin, D., Li, A., Deng, L., Dong, A., Zhang, J., 2025. A zwitterionic polymer filtrate reducer with enhanced anti-polyelectrolyte effect for high-temperature and high-salinity conditions. Chem. Eng. J. 508. https://doi.org/10.1016/j.cej.2025.161087.
Gautam, S., Guria, C., Rajak, V.K., 2022. A state of the art review on the performance of high-pressure and high-temperature drilling fluids: Towards understanding the structure-property relationship of drilling fluid additives. J. Petrol. Sci. Eng. 213. https://doi.org/10.1016/j.petrol.2022.110318.
Gautam, S., Kumar, S., Kumar, A., Rajak, V.K., Guria, C., 2025. Development of functional polymer-based clay-free HPHT drilling fluid: Effect of molecular weight and its distribution on drilling fluid performance. Geoenergy Sci. Eng. 246. https://doi.org/10.1016/j.geoen.2024.213616.
Greesh, N., Hartmann, P.C., Cloete, V., Sanderson, R.D., 2008. Adsorption of 2-acrylamido-2-methyl-1-propanesulfonic acid (AMPS) and related compounds onto montmorillonite clay. J. Colloid Interface Sci. 319 (1), 2–11. https://doi.org/10.1016/j.jcis.2007.10.019.
Huo, J.H., Peng, Z.G., Ye, Z.B., Feng, Q., Zheng, Y., Zhang, J., Liu, X.J., 2018. Preparation, characterization, and investigation of poly(AMPS/AM/SSS) on application performance of water-based drilling fluid. J. Appl. Polym. Sci. 135 (29). https://doi.org/10.1002/app.46510.

Jamadagni, S.N., Godawat, R., Garde, S., 2009. How surface wettabitity affects the binding, folding, and dynamics of hydrophobic polymers at interfaces. Langmuir 25 (22), 13092–13099. https://doi.org/10.1021/la9011839.
Jiang, G., He, Y., Cui, W., Yang, L., Ye, C., 2019. A saturated saltwater drilling fluid based on salt-responsive polyampholytes. Petrol. Explor. Dev. 46 (2), 385–390. https://doi.org/10.1016/S1876-3804(19)60020-0.
Ju, Z.H., Brosse, N., Hoppe, S., Wang, Z.Q., Ziegler-Devin, I., Zhang, H.Y., Shu, B.Q., 2024. Thermal and mechanical properties of polyethylene glycol (PEG)-modified lignin/polylactic acid (PLA) biocomposites. Int. J. Biol. Macromol. 262. https://doi.org/10.1016/j.ijbiomac.2024.129997.
Koh, J.K., Lai, C.W., Johan, M.R., Gan, S.S., Chua, W.W., 2022. Recent advances of modified polyacrylamide in drilling technology. J. Petrol. Sci. Eng. 215. https://doi.org/10.1016/j.petrol.2022.110566.
Lattimer, R.P., Williams, R.C., 2002. Low-temperature pyrolysis products from a polyether-based urethane. J. Anal. Appl. Pyrolysis 63 (1), 85–104. https://doi.org/10.1016/s0165-2370(01)00143-7.
Li, A., Gao, S., Zhang, G., Zeng, Y., Hu, Y., Zhai, R., Dong, A., Zhang, J., 2024. A review in polymers for fluid loss control in drilling operations. Macromol. Chem. Phys. 225 (8). https://doi.org/10.1002/macp.202300390.
Li, H., Liu, F., Sun, J.S., Wang, R., Hao, H.J., Huang, X.B., 2025. Performance and mechanism study of ampholytic copolymer as a temperature-resistant and salt-tolerant filtration loss control additive in water-based drilling fluids. Colloids Surf. A Physicochem. Eng. Asp. 722. https://doi.org/10.1016/j.colsurfa.2025.137235.
Lin, L., Li, X., Shi, C.L., Mao, Y.F., 2019. Desorption of hydrolyzed poly(AM/DMDAAC) from bentonite and its decomposition in saltwater under high temperatures. E-Polymers 19 (1), 527–534. https://doi.org/10.1515/epoly-2019-0056.
Lin, Z., Li, F., Liu, X., Su, J., 2024. High temperature degradable pullulan microsphere/polymer composite for filtration loss control of water-based drilling fluids. Geoenergy Sci. Eng. 243. https://doi.org/10.1016/j.geoen.2024.213362.
Liu, J.P., Zhang, T.F., Sun, Y.W., Lin, D., Feng, X., Wang, F.C., 2022. Insights into the high temperature-induced failure mechanism of bentonite in drilling fluid. Chem. Eng. J. 445. https://doi.org/10.1016/j.cej.2022.136680.
Liu, L.M., Sun, J.S., Wang, R., Liu, F., Gao, S.F., Yang, J., Ren, H., Qu, Y.Z., Cheng, R.C., Geng, Y., Feng, Z.B., 2022a. New zwitterionic polymer as a highly effective salt- and calcium-resistant fluid loss reducer in water-based drilling fluids. Gels 8 (11). https://doi.org/10.3390/gels8110735.
Liu, L.M., Sun, J.S., Wang, R., Qu, Y.Z., Liu, F., Yang, J., Cheng, R.C., Gao, S.F., Huang, H. J., 2022b. Synthesis of a new high temperature and salt resistant zwitterionic filtrate reducer and its application in water-based drilling fluid. Colloids Surf. A Physicochem. Eng. Asp. 651. https://doi.org/10.1016/j.colsurfa.2022.129730.
Liu, P., 2007. Polymer modified clay minerals: A review. Appl. Clay Sci. 38 (1–2), 64–76. https://doi.org/10.1016/j.clay.2007.01.004.
Luo, Y.H., Lin, L., Guo, Y.J., Luo, P.Y., Xiong, G.X., Li, Z., Ao, H.D., 2023. Study on high-temperature degradation of acrylamide-based polymer ZP1 in aqueous solution. Polym. Degrad. Stabil. 217. https://doi.org/10.1016/j.polymdegradstab.2023.110533.
Mao, H., Wang, W.J., Ma, Y.L., Huang, Y., 2021. Synthesis, characterization and properties of an anionic polymer for water-based drilling fluid as an anti-high temperature and anti-salt contamination fluid loss control additive. Polym. Bull. 78 (5), 2483–2503. https://doi.org/10.1007/s00289-020-03227-y.
Matsuoka, S., Kawamoto, H., Saka, S., 2012. Retro-aldol-type fragmentation of reducing sugars preferentially occurring in polyether at high temperature: Role of the ether oxygen as a base catalyst. J. Anal. Appl. Pyrolysis 93, 24–32. https://doi.org/10.1016/j.jaap.2011.09.005.
Mech, D., Sangwai, J.S., 2016. Effect of molecular weight of polyethylene glycol (PEG), a hydrate inhibitive water-based drilling fluid additive, on the formation and dissociation kinetics of methane hydrate. J. Nat. Gas Sci. Eng. 35, 1441–1452. https://doi.org/10.1016/j.jngse.2016.06.020.
Minakov, A.V., Pryazhnikov, M.I., Mikhienkova, E.I., Voronenkova, Y.O., 2023. Systematic experimental study of the temperature dependence of viscosity and rheological behavior of water-based drilling fluids with nano-additives. Petroleum 9 (4), 534–544. https://doi.org/10.1016/j.petlm.2022.03.001.
Noor, A.A., Khan, M.A., Zhang, Y., Lv, K., Sun, J., Liu, C., Li, M.-C., 2025. Modified natural polymers as additives in high-temperature drilling fluids: A review. Int. J. Biol. Macromol. 287. https://doi.org/10.1016/j.ijbiomac.2024.138556.
Obi, C.E., Hasan, A.R., Rahman, M.A., Banerjee, D., 2024. Multiphase flow challenges in drilling, completions, and injection: Part 1. Petroleum 10 (4), 557–569. https://doi.org/10.1016/j.petlm.2024.05.001.
Oya, Y., Kawakatsu, T., 2014. Soft confinement for polymer solutions. Europhys. Lett. (2). https://doi.org/10.1209/0295-5075/107/28003.
Pollak, E., 2024. Instanton-based Kramers turnover theory. Phys. Rev. 109 (2). https://doi.org/10.1103/PhysRevA.109.022242.
Pollak, E., Miret-Artes, S., 2023. Recent developments in Kramers' theory of reaction rates. ChemPhysChem 24 (16). https://doi.org/10.1002/cphc.202300272.
Qu, Y.Z., Zhang, W.C., Ren, H., Yuan, Y.H., Zhou, X.Y., Yang, G., Zhang, X.F., 2024. Investigation of the correlation between molecular structures with high-temperature and salt resistance for acrylamides polymer in drilling fluid. J. Dispersion Sci. Technol. 45 (7), 1364–1372. https://doi.org/10.1080/01932691.2023.2211136.
Song, X., Li, G., Huang, Z., Shi, Y., Wang, G., Song, G., Xu, F., 2023. Review of high-temperature geothermal drilling and exploitation technologies. Gondwana Res. 122, 315–330. https://doi.org/10.1016/j.gr.2022.10.013.
Sun, J., Huang, X., Lu, K., Shao, Z., Meng, X., Wang, J., Li, W., 2019. Methods, technical progress and research advance of improving high-temperature stability of water based drilling fluids. J. China Univ. Petrol. Edit. Natr. Sci. 43 (5), 73–81 (in Chinese).
Sun, J., Lei, S., Bai, Y., Lu, K., Zhang, S., Han, J., Cheng, R., Liu, F., 2021. Mechanical transformation mechanism of polymer materials and its application prospects in the field of drilling fluids. Acta Pet. Sin. 42 (10), 1382–1394 (in Chinese).
Sun, J., Zhang, X., Lv, K., Liu, J., Xiu, Z., Wang, Z., Huang, X., Bai, Y., Wang, J., Jin, J., 2022. Synthesis of hydrophobic associative polymers to improve the rheological and filtration performance of drilling fluids under high temperature and high salinity conditions. J. Petrol. Sci. Eng. 209. https://doi.org/10.1016/j.petrol.2021.109808.
Sun, J., Sun, Y., Lai, Y., Li, L., Yang, G., Lv, K., Zhang, T., Zhang, X., Wang, Z., Xu, Z., Dai, Z., Liu, J., 2024a. Progress in the application of graphene material in oilfield chemistry: A review. Petroleum 10 (2), 175–190. https://doi.org/10.1016/j.petlm.2023.12.002.
Sun, J., Yang, J., Bai, Y., Lyu, K., Liu, F., 2024b. Research progress and development of deep and ultra-deep drilling fluid technology. Petrol. Explor. Dev. 51 (4), 889–898. https://doi.org/10.1016/S1876-3804(24)60522-7.
Sun, Y.W., Sun, J.S., Li, L., Lv, K.H., Zhang, X.F., Wang, Z.L., Dai, Z.W., Xu, Z., Zhang, T.F., Liu, J.P., 2023. Development of high-temperature and high-mineralization-resistant adaptive plugging agent and its performance evaluation. Energy & Fuels 37 (13), 8999–9010. https://doi.org/10.1021/acs.energyfuels.3c01306.
Tang, X., Yuan, B., Yang, Y., Xie, Y., 2016. Preparation and performance of AMPS/AA/DMAA/SA copolymer as a filtrate reducer for oil well cementing. J. Appl. Polym. Sci. 133 (33). https://doi.org/10.1002/app.43824.
Wang, D.-Y., Chen, C.-F., Ju, F., Ke, Y.-C., 2024. High-temperature resistant polymer nanocomposites with exfoliated organic-modified montmorillonite nanosheets strongly adsorbed on polymer chains. Pet. Sci. 21 (5), 3630–3643. https://doi.org/10.1016/j.petsci.2024.07.006.
Wang, F.H., Tan, X.C., Wang, R.H., Sun, M.B., Wang, L., Liu, J.H., 2012. High temperature and high pressure rheological properties of high-density water-based drilling fluids for deep wells. Pet. Sci. 9 (3), 354–362. https://doi.org/10.1007/s12182-012-0219-4.
Wang, L., Wang, D., Bao, W., 2013. Effect of clay on polycarboxylate superplasticizer performance and mechanism research. J. Wuhan Univ. Technol. 35 (8), 6–9 (in Chinese).
Wang, R., Deng, Y.L., Yang, J., Sun, J.S., Shan, W.J., Tao, H.Z., Wang, J.L., Liu, L.M., Yang, Z.X., Ren, H., 2024. Preparation of a salt-responsive zwitterionic hydrophobically associating polymer and its application in a saturated sodium chloride drilling fluid. Colloids Surf. A Physicochem. Eng. Asp. 692. https://doi.org/10.1016/j.colsurfa.2024.133956.
Wang, R., Han, K., Li, Y., Jin, C., 2022. A novel anti-clay silane-modified polycarboxylate superplasticizer: Preparation, performance and mechanism. Constr. Build. Mater. 33, 1. https://doi.org/10.1016/j.conbuildmat.2022.127311.
Wisniowski, R., Skrzypaszek, K., Malachowski, T., 2020. Selection of a suitable rheological model for drilling fluid using applied numerical methods. Energies 13 (12). https://doi.org/10.3390/en13123192.
Wu, X., Niu, X., Gao, Q., Fan, Y., 2018. Effect of polycarboxylate superplasticizers containing AMPS on clay sensitivity. J. Build. Mater. 21 (1), 15–19+25 (in Chinese).
Xie, G., Luo, Y., Wang, C., Deng, M., Bai, Y., 2023. Comparative study on the inhibiting mechanism of inhibitor with primary amine groups and quaternary ammonium groups for sodium bentonite. Petroleum 9 (4), 526–533. https://doi.org/10.1016/j.petlm.2022.05.001.
Xie, T., Huo, L.L., Yao, Z.L., Zhang, X.Y., Liu, Z.Y., Jia, J.X., Zhao, Y.N., Zhao, L.X., 2024. Co-pyrolysis of biomass and polyethylene: Mechanistic insights into functional group transformations on solid matrix. Chem. Eng. J. 482. https://doi.org/10.1016/j.cej.2024.149166.
Xiong, L., Zheng, G., Bi, Y., Fu, C., 2015. Effect of typical clay upon the dispersion performance of polycarboxylate superplasticizer. In: 2015 International Conference on Materials, Environmental and Biological Engineering. Atlantis Press, pp. 226–229.
Xu, W.S., Douglas, J.F., Freed, K.F., 2016. Generalized entropy theory of glass-formation in fully flexible polymer melts. J. Chem. Phys. 145 (23). https://doi.org/10.1063/1.4972412.
Yan, L.L., Wang, C.B., Xu, B., Sun, J.S., Yue, W., Yang, Z.X., 2013. Preparation of a novel amphiphilic comb-like terpolymer as viscosifying additive in low-solid drilling fluid. Mater. Lett. 105, 232–235. https://doi.org/10.1016/j.matlet.2013.04.025.
Yang, J., Wang, R., Sun, J.S., Wang, J.L., Liu, L.M., Qu, Y.Z., Wang, P.Q., Ren, H., Gao, S., Yang, Z.X., 2023. Nanolaponite/comb polymer composite as a rheological modifier for water-based drilling fluids. ACS Appl. Nano Mater. 6 (14), 13453–13465. https://doi.org/10.1021/acsanm.3c02079.
Yang, J., Sun, J.S., Wang, R., Qu, Y.Z., Liu, F., Feng, X.H., Wang, H.H., Yang, Z.X., Ren, H., Liu, L.M., 2024. Investigation of TPEG comb polymer as filtration and rheological additives for high-temperature water-based drilling fluid. J. Mol. Liq. 400. https://doi.org/10.1016/j.molliq.2024.124577.
Yang, X.J., Xiong, Z.G., Mao, J.C., Yang, T., Fu, B., Han, D.F., Yang, J.X., Chen, W., Liu, W., Zhang, Q., Xiao, S.Y., Zhang, Y., Lin, C., 2024. Molecular dynamics simulations to study the adsorption damage of modified polyacrylamide in sandstone pores. J. Mol. Liq. 397. https://doi.org/10.1016/j.molliq.2024.124096.
Yao, F., Li, M., Pan, L., Li, J., Xu, N., 2022. Synthesis of sodium alginate-polycarboxylate superplasticizer and its tolerance mechanism on montmorillonite. Cement Concr. Compos. 133. https://doi.org/10.1016/j.cemconcomp.2022.104638.
Zang, J.L., Sun, W., Yang, Z.K., Ding, Z.J., Dong, M., Jiang, S.J., Gui, Y.H., Jia, H.L., 2025. Experimental study on thermokinetic characteristics of multiple coal seams in

Xinjiang open pit mine using thermogravimetric-Fourier transform infrared spectroscopy and thermogravimetric-mass spectrometry. Thermochim. Acta 747. https://doi.org/10.1016/j.tca.2025.179973.

Zhang, J.R., Xu, M.D., Christidis, G.E., Zhou, C.H., 2020. Clay minerals in drilling fluids: Functions and challenges. Clay Miner. 55 (1), 1–11. https://doi.org/10.1180/clm.2020.10.

Zhang, L.L., Cao, J.Z., 2019. Pyrolysis and its mechanism of organomontmorillonite (OMMT) influenced by different functional groups. J. Therm. Anal. Calorim. 137 (1), 1–10. https://doi.org/10.1007/s10973-018-7947-7.

Zheng, W., Wu, X., Huang, Y., 2020. Impact of polymer addition, electrolyte, clay and antioxidant on rheological properties of polymer fluid at high temperature and high pressure. J. Pet. Explor. Prod. Technol. 10 (2), 663–671. https://doi.org/10.1007/s13202-019-0732-8.

Zhong, H.Y., Huang, W.A., Qiu, Z.S., Cao, J., Xie, B.Q., Wang, F.W., Zheng, W., 2015. Inhibition comparison between polyether diamine and formate salts as shale inhibitor in water-based drilling fluid. Energy Sources, Part A Recovery, Util. Environ. Eff. 37 (18), 1971–1978. https://doi.org/10.1080/15567036.2011.654315.

Zhong, H., Gao, X., Qiu, Z., Sun, B., Huang, W., Li, J., 2020. Insight into β-cyclodextrin polymer microsphere as a potential filtration reducer in water-based drilling fluids for high temperature application. Carbohydr. Polym. 249. https://doi.org/10.1016/j.carbpol.2020.116833.

Zuo, W.Q., Feng, P., Zhong, P.H., Tian, Q., Gao, N.X., Wang, Y.J., Yu, C., Miao, C.W., 2017. Effects of novel polymer-type shrinkage-reducing admixture on early age autogenous deformation of cement pastes. Cement Concr. Res. 100, 413–422. https://doi.org/10.1016/j.cemconres.2017.08.007.